

XVIII TAUP CONFERENCE

Status of the HENSA collaboration at the Canfranc Underground Laboratory: results from two years measurement of the neutron flux in hall B

Nil Mont-Geli

Institut de Tècniques Energètiques
Universitat Politècnica de Catalunya
nil.mont@upc.edu

Ariel Tarifeño-Saldivia

Instituto de Física Corpuscular
C.S.I.C – Universidad de Valencia
atarisal@ific.uv.es



UNIVERSITAT POLITÈCNICA DE CATALUNYA
BARCELONATECH

Institut de Tècniques Energètiques



LSC
Laboratorio Subterráneo de Canfranc

IFIC
INSTITUT DE FÍSICA
CORPUSCULAR

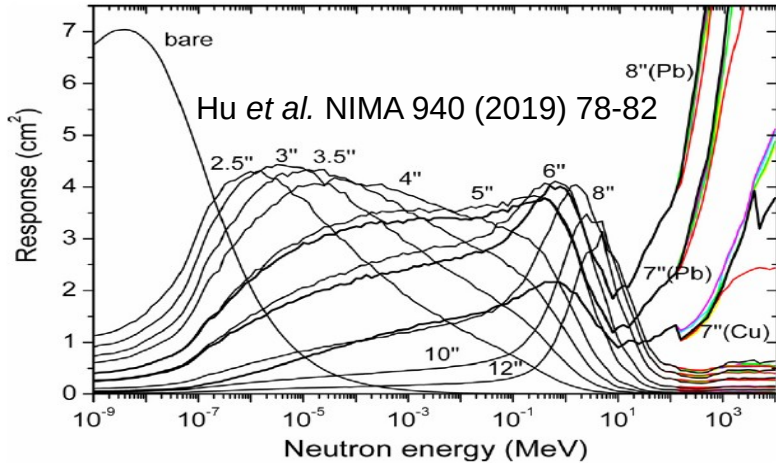
CSIC
CONSEJO SUPERIOR DE INVESTIGACIONES CIENTÍFICAS

Objectives

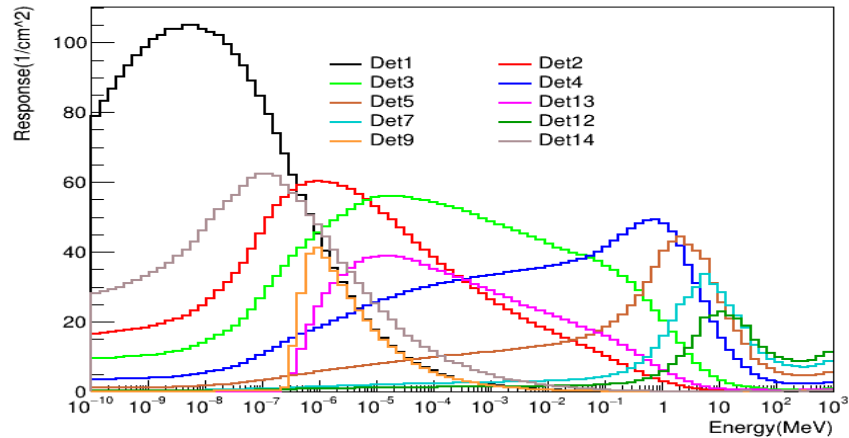
- Understand the neutron sources.
(simulations)
- Characterization of the temporal evolution of the neutron flux.
(monitoring rates)
- Characterization of neutron flux energy spectrum.
(spectra reconstruction)

The High Efficiency Neutron Spectrometry Array

Standard extended Bonner Spheres



HENSA version LSC-2022



HENSA neutron response is **~5-15 times larger** than standard Bonner Spheres systems.

Neutron sensitivity from thermal up to 20 MeV.

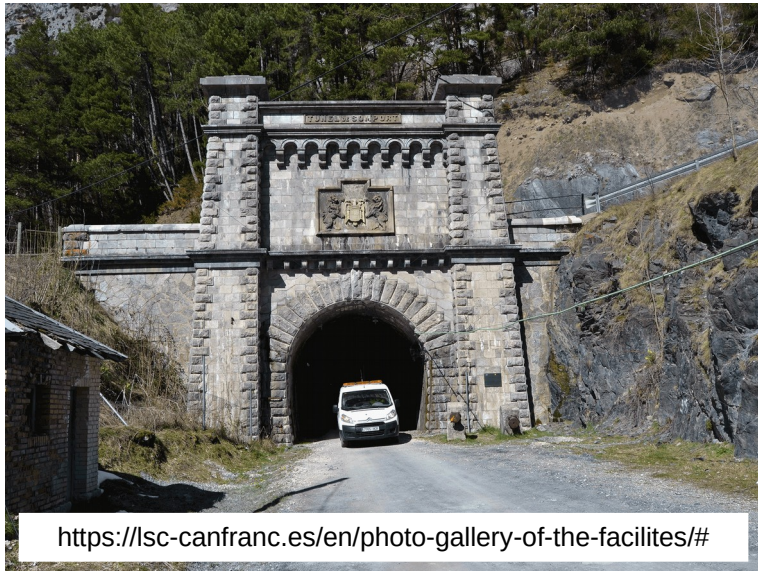
Use of **larger counters** (3He) and of moderators (HDPE) with the shape of a rectangular prisms.



The Canfranc Underground Laboratory (LSC)

The Canfranc Underground Laboratory (LSC) is located under Mount Tobazo in the Aragonese Pyrenees (Spain).

- Three experimental halls (A, B and C).
- 2450 mwe (meters water equivalent) depth.
- Underground research: nuclear physics, dark matter, neutrino physics, geology, biology, cryogenics



Laboratorio Subterráneo de Canfranc

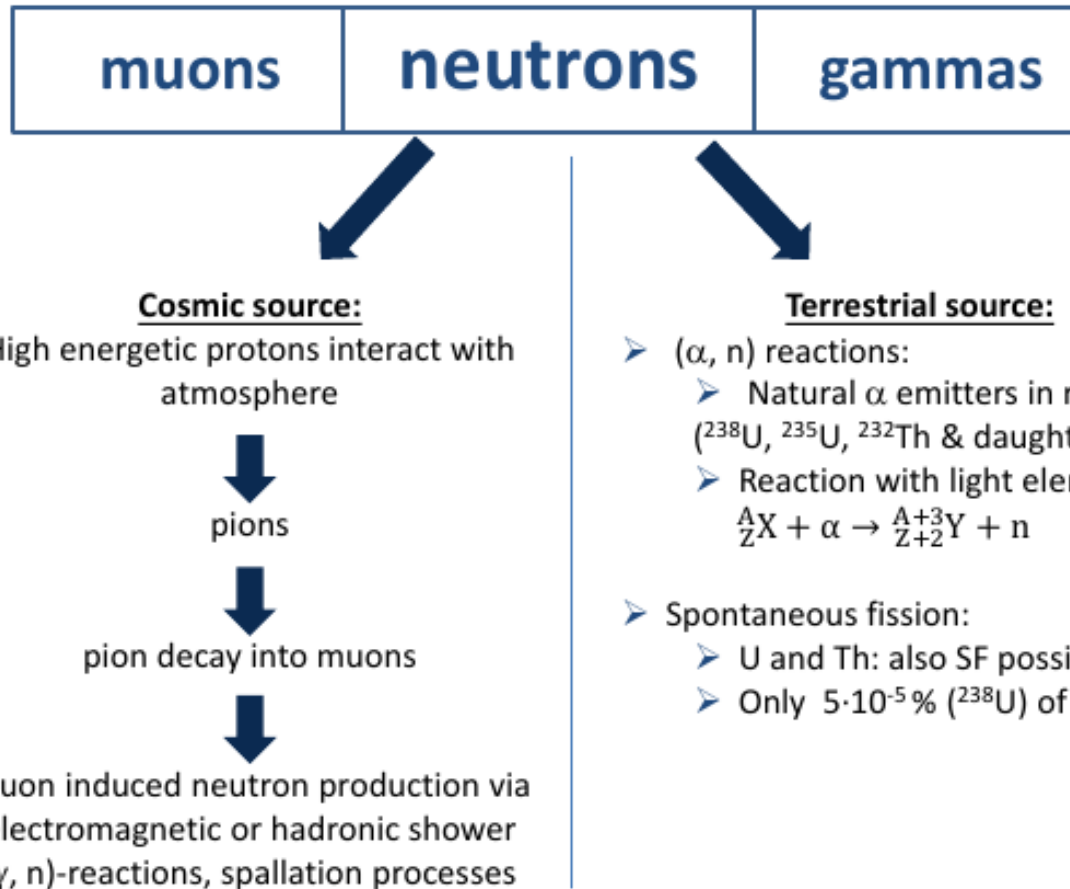


The HENSA project

- Short-term measurement at LSC (empty hall A):
D. Jordan et al 2013, Astroparticle Physics 42, 1 – 6
Corrigendum: D. Jordan et al 2020, Astroparticle Physics 118, 102372
- Measurement at Felsenkeller:
M. Grieger et al 2020, Phys. Rev. D 101, 123027
- Long-term campaign in hall A of the LSC (October 2019 – March 2021):
S. Orrigo et al 2022, European Physics Journal C 82, 814
- Cosmic rays campaign (July - August and October 2020).
- Long-term campaign in hall B of the LSC (since March 2021): **THIS TALK**
N. Mont-Geli et al 2021, Journal of Physics: Conference Series 2156, 012223
- Continuous monitoring with a reduced setup (4 detectors) in hall A:
Ph. D. Thesis by J. Plaza (CIEMAT)

Simulations of the neutron flux

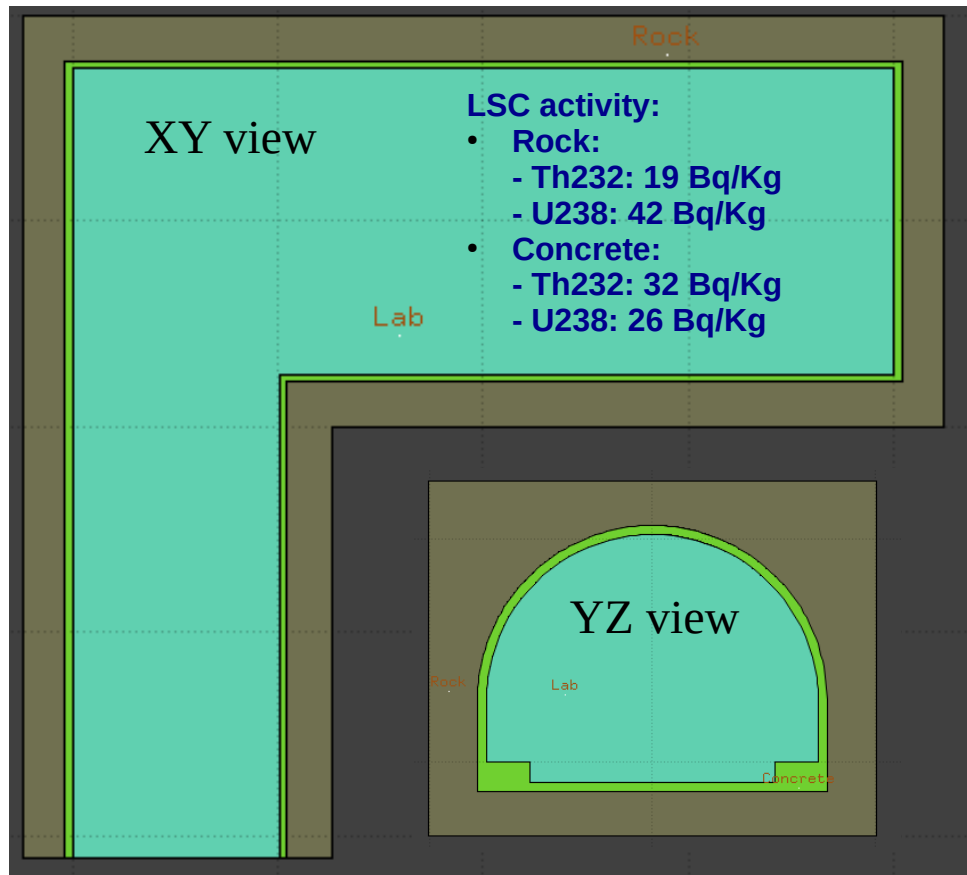
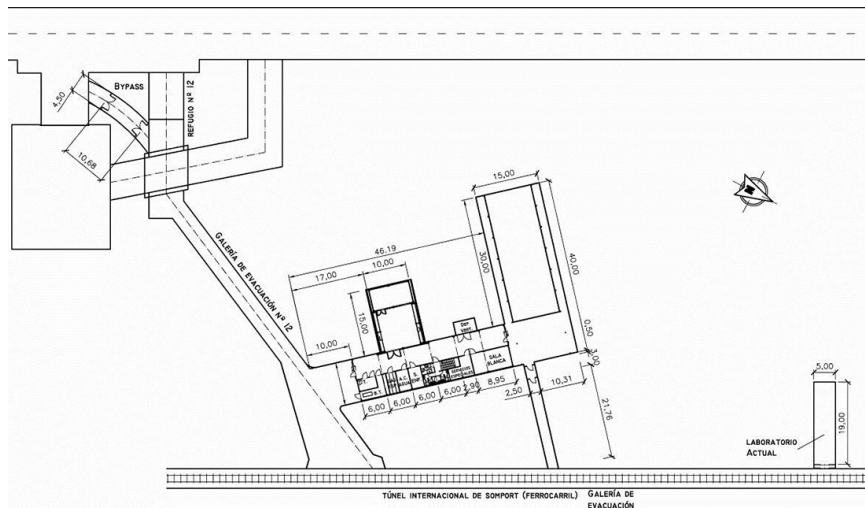
Neutron flux in underground laboratories



Monte Carlo simulations of the neutron flux

The Canfranc Underground laboratory (**hall A**).

- 15 x 40 m² ground plan.
 - ~ 13 m roof altitude.
 - Between the rock and the laboratory halls there is a ~40 cm thickness lay of concrete (**concrete walls**).



Monte Carlo simulations of the neutron flux

Monte Carlo FLUKA (v. 4.3.2) calculations used to estimate the neutron flux in Canfranc.

- (α, n) reactions.
- Spontaneous fission.
- Thermal peak $\sim 4.5 - 6.5 \cdot 10^{-8}$ MeV
- Isolethargic intermediate region
- Fast peak $\sim 0.5 - 3$ MeV (1 MeV P and LS)

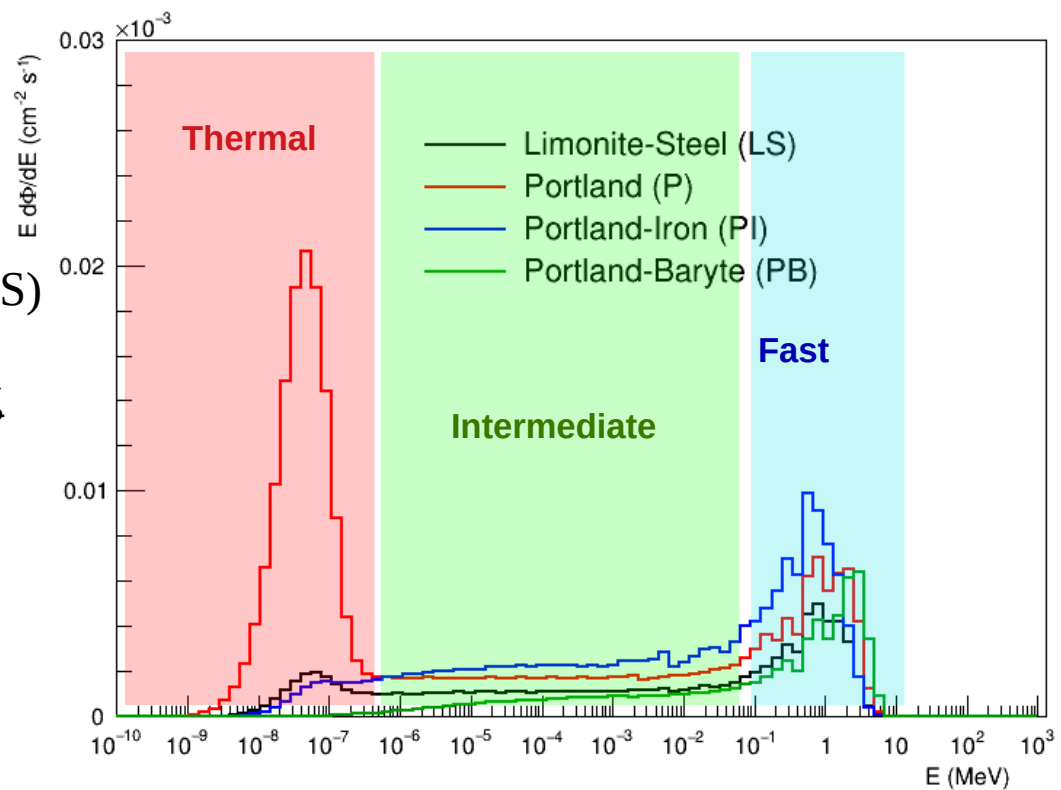
Spectra to be used as priors in the unfolding algorithms.

For Portland concrete:

- Concrete contribution: 94%.
- Rock contribution: 6%.

Based in the work by M. Grieger at Felsenkeller:

M. Grieger et al 2020, Phys. Rev. D 101, 123027



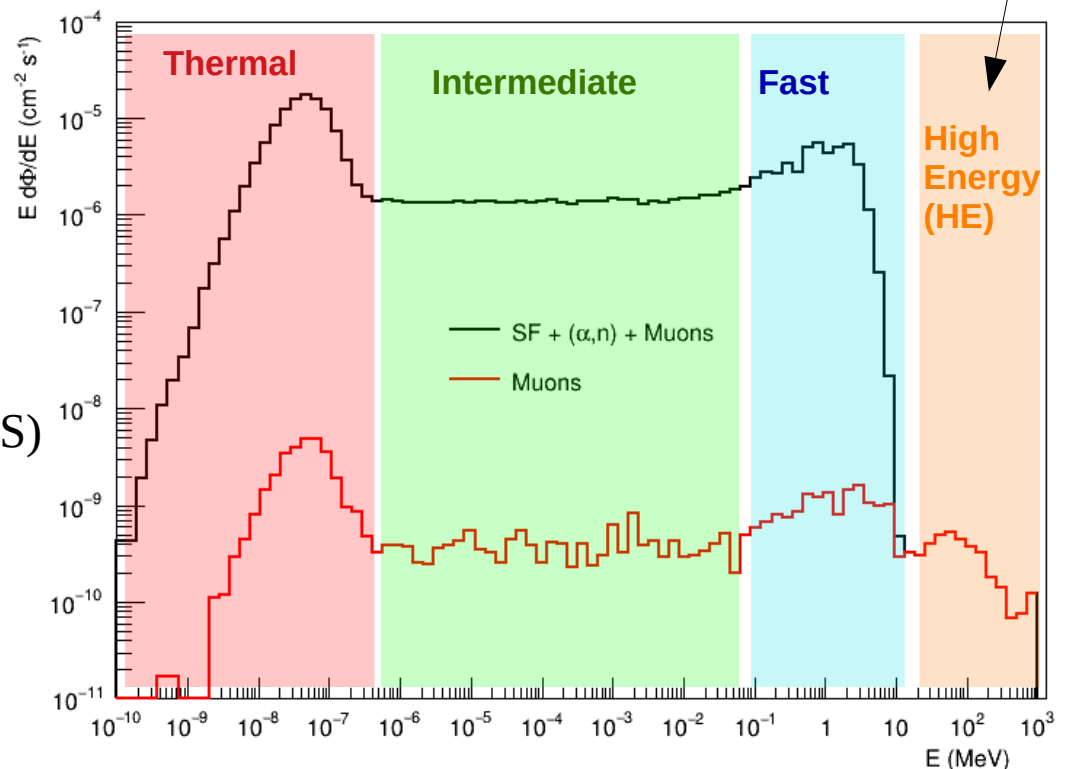
Monte Carlo simulations of the neutron flux

Monte Carlo FLUKA (v. 4.3.2) calculations used to estimate the neutron flux in Canfranc.
(ex: Portland concrete)

not feasible
with HENSA

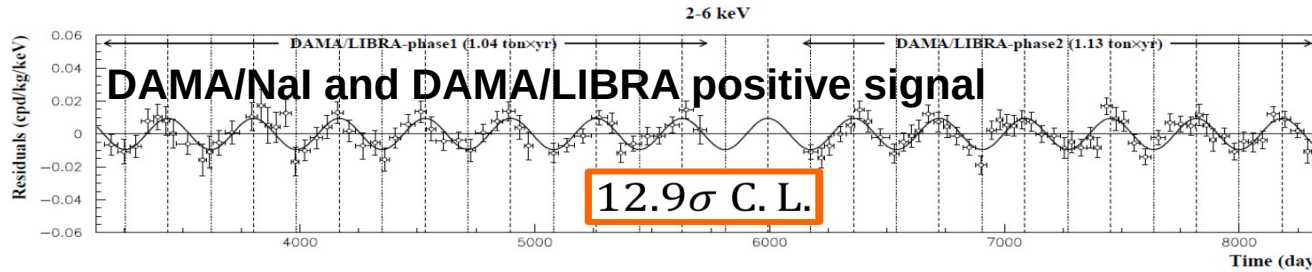
- (α,n) reactions.
- Spontaneous fission.
- **Muon-induced neutrons**
- Thermal peak $\sim 4.5 - 6.5 \cdot 10^{-8}$ MeV
- Isolethargic intermediate region
- Fast peak $\sim 0.5 - 3$ MeV (1 MeV P and LS)
- HE peak ~ 50 MeV
- **Muons contribution: 0.03%.**
**Preliminary estimation*

Based in the work by M. Grieger at Felsenkeller:
M. Grieger et al 2020, Phys. Rev. D 101, 123027



HENSA in hall B

Physical case (ANALIS - 112)



See talks by:

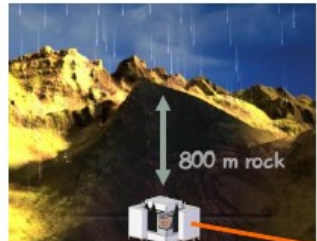
- Tamara Pardo (30 Aug, 14:30)
- Iván Coarasa (31 Aug, 16:15)

Goal

ANALIS (*Annual modulation with Nal(Tl) scintillators*) intends to provide a **model independent** test of the signal reported by DAMA/LIBRA, using the **same target and technique** at the **Canfranc Underground Laboratory** (Spain)



Centro de Astropartículas y
Física de Altas Energías
Universidad Zaragoza



Experimental goals

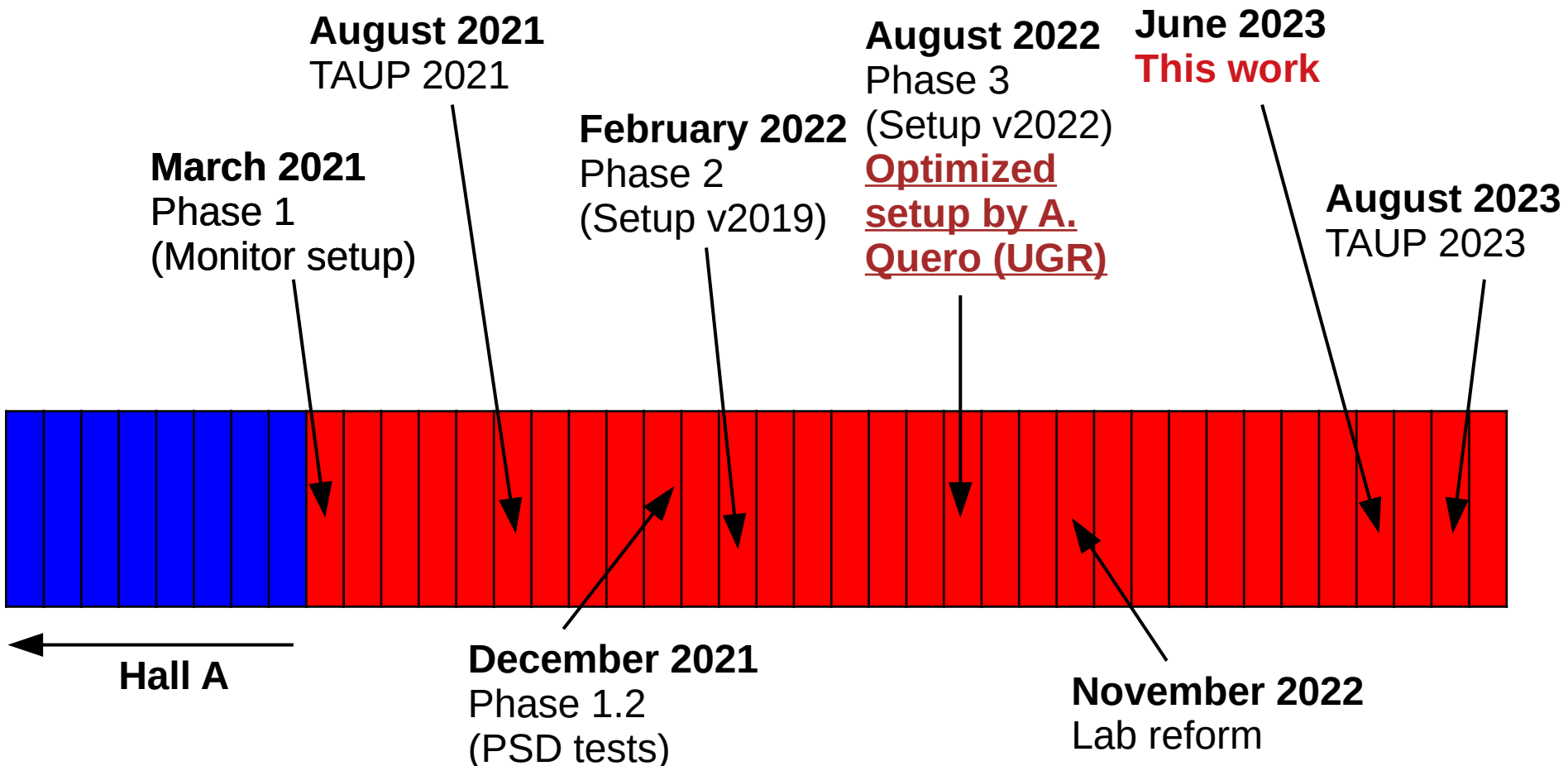
- Energy **threshold** at 1 keV_{ee}
- **Background** level below 10 keV_{ee} at a few cpd/kg/keV_{ee}
- Very **stable** operation conditions

Courtesy ANAIS team

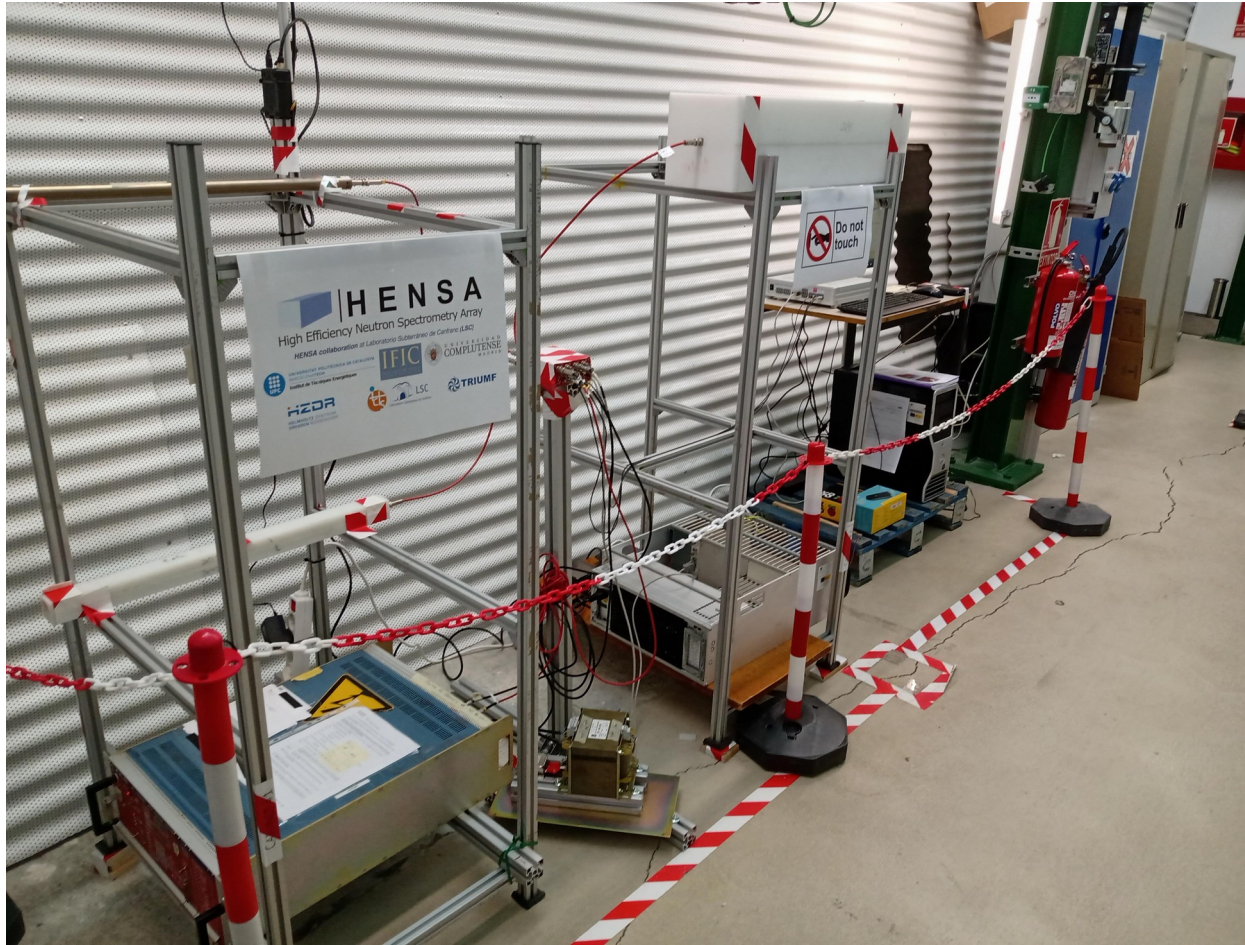
For ANALIS is **relevant** the measurement of:

- I) total **neutron flux** and spectral distribution at LSC (Hall B).
- II) Possible **long-term variations** of the neutron flux. Required in order to set a limit on the corresponding effect in ANALIS background and annual modulation analysis.

Experimental campaign in hall B



Experimental setup in phase 1 (monitor)



Experimental setup in phase 2 (v 2019)



Response matrix (v 2019)

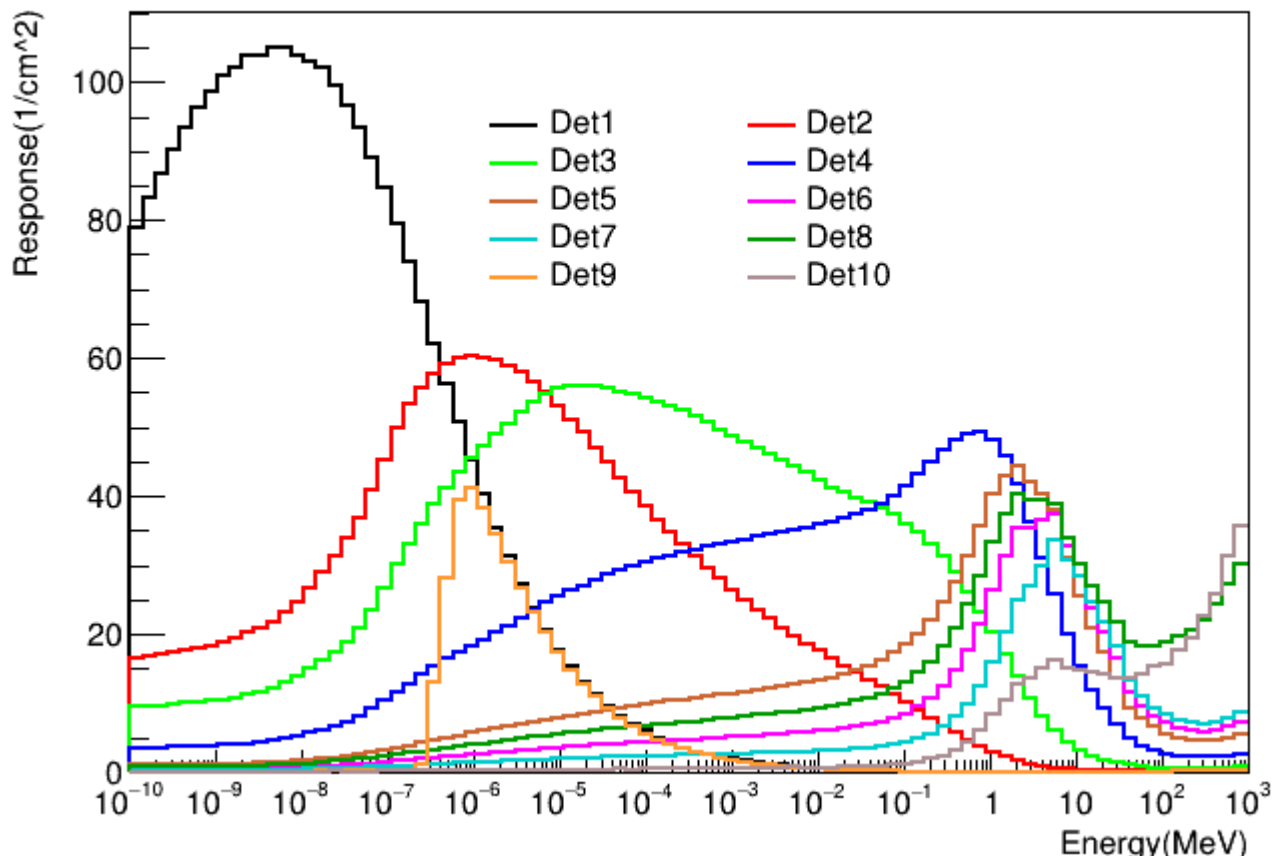
Version 2019

Monte Carlo calculations using Particle Counter, code based on Geant 4.

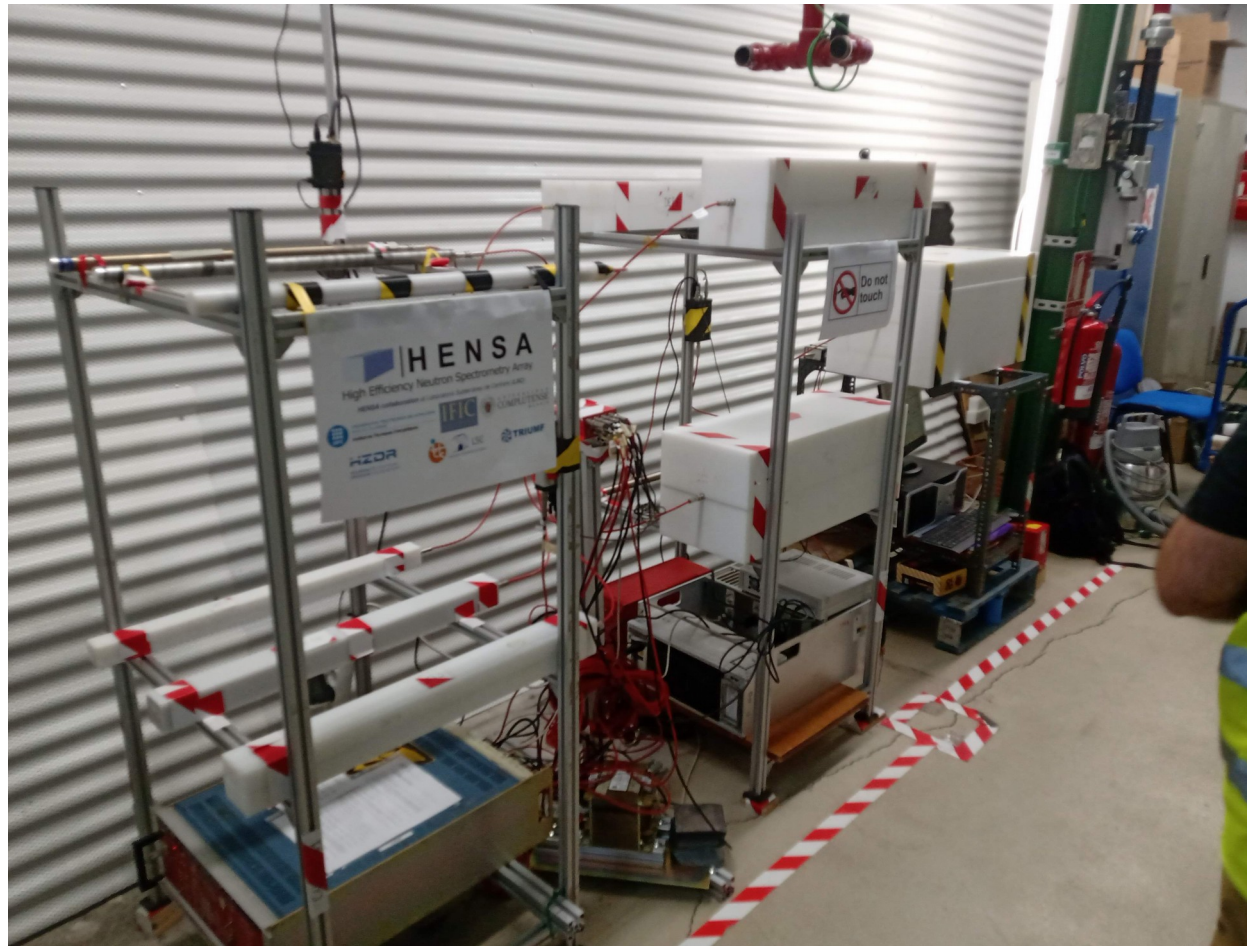
Vacuum independent detectors.



<https://www.particlecounter.net>



Experimental setup in phase 3 (v 2022)



Response matrix (v 2022)

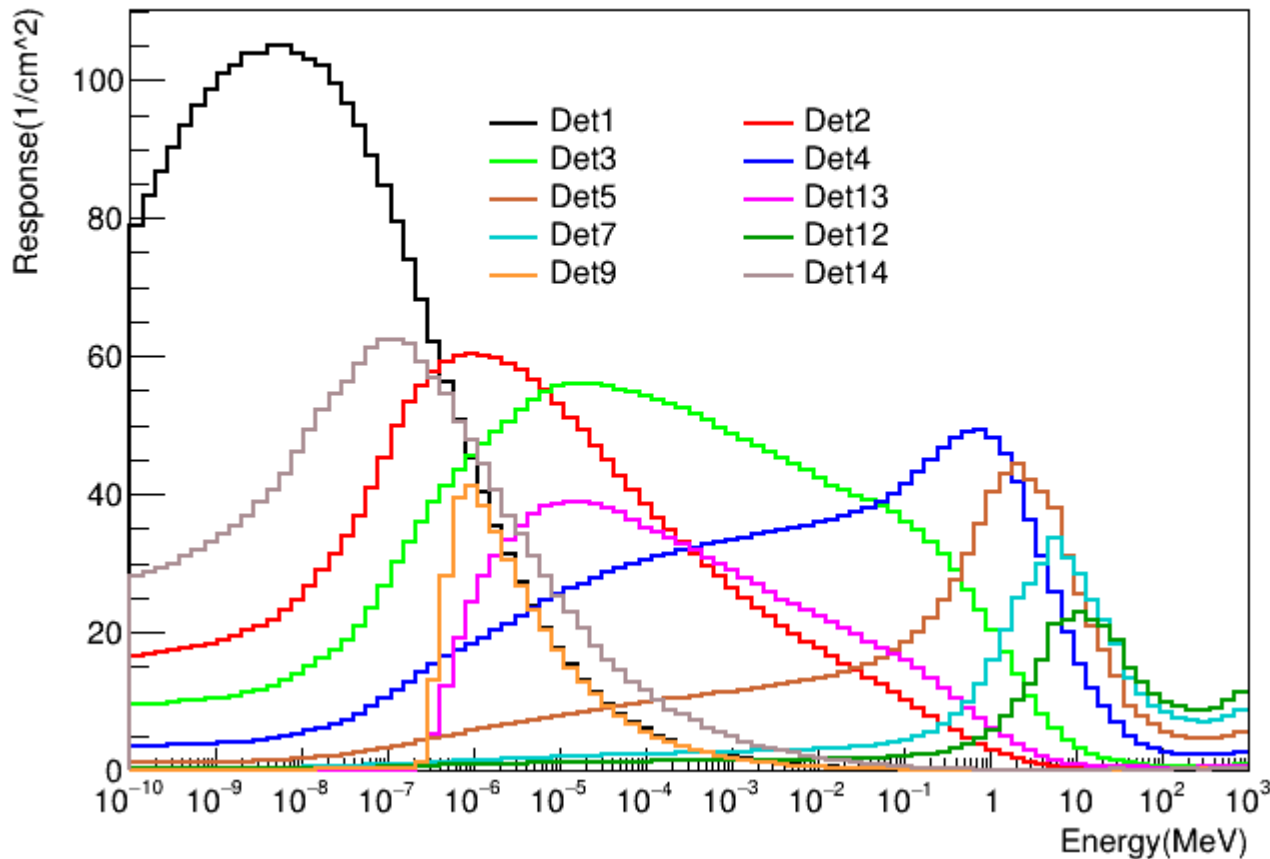
Version 2022

New design with improved spectral resolution by **A. Quero (UGR)**.

Vacuum independent detectors



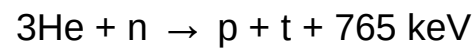
<https://www.particlecounter.net>



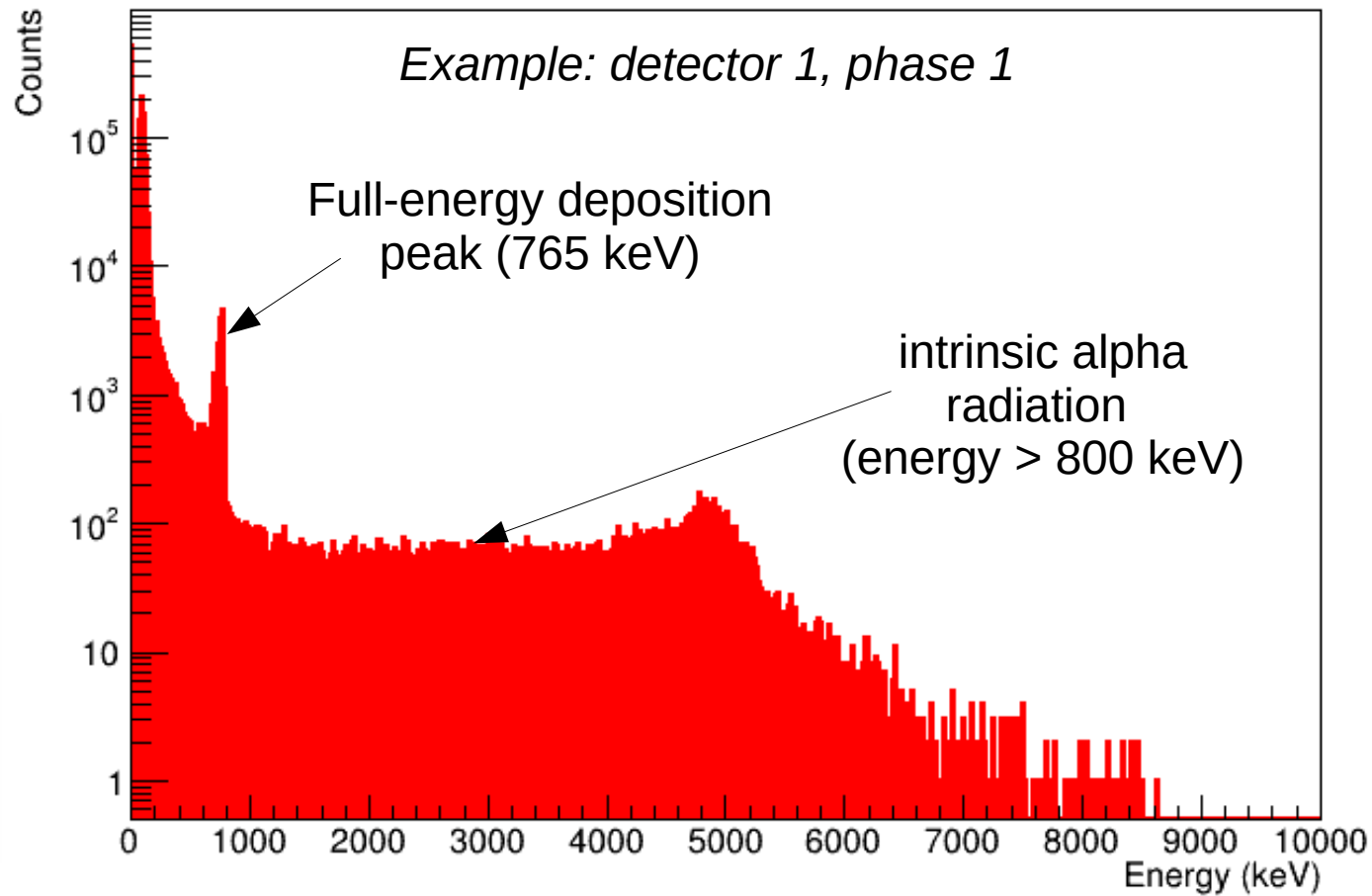
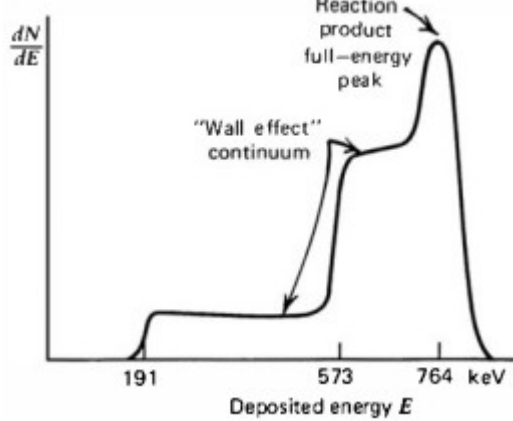
Data analysis

^3He counter energy deposition spectrum (event amplitude)

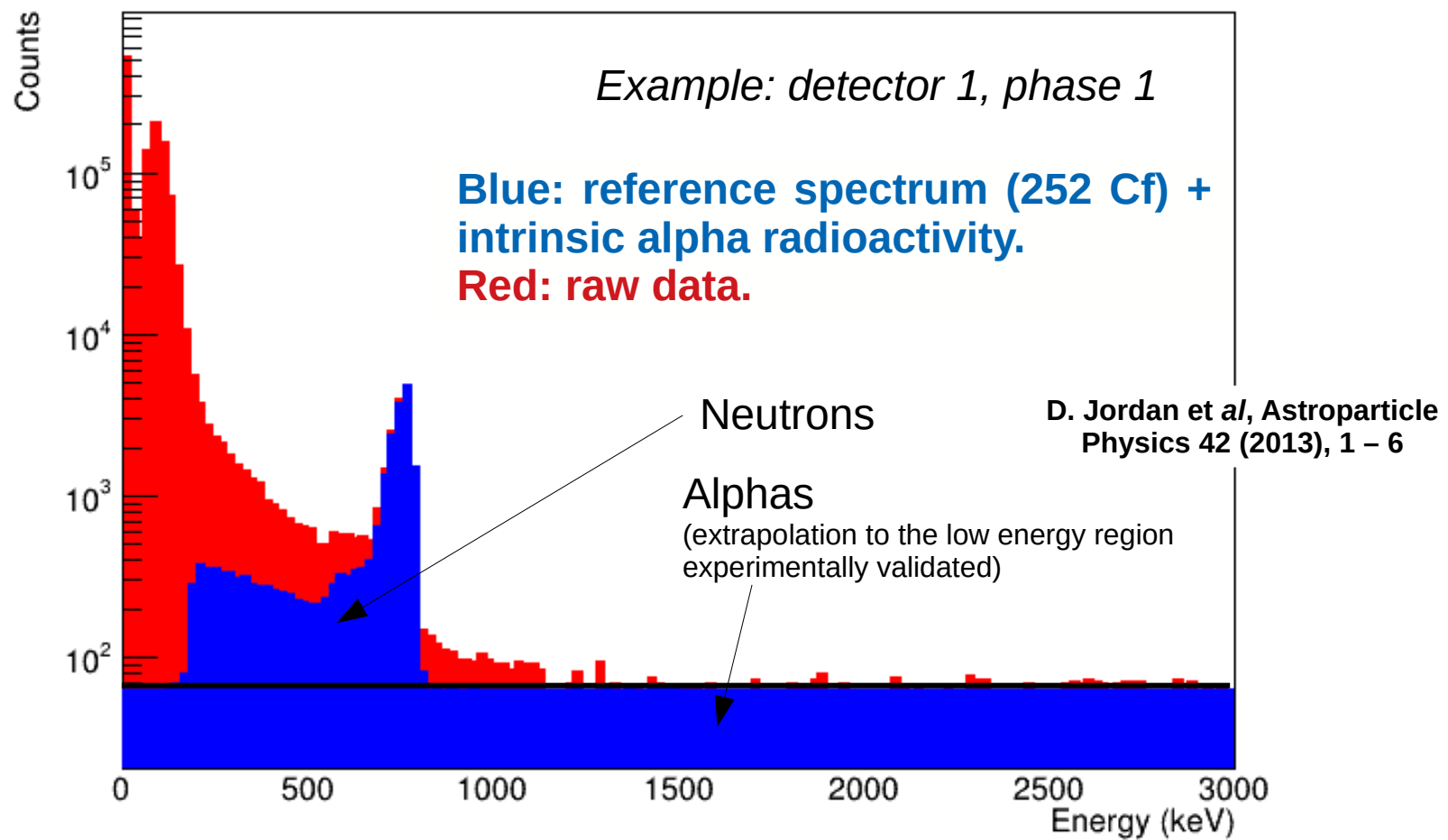
Raw data



Theoretical amplitude spectrum
(G. Knoll, 2010 edition)

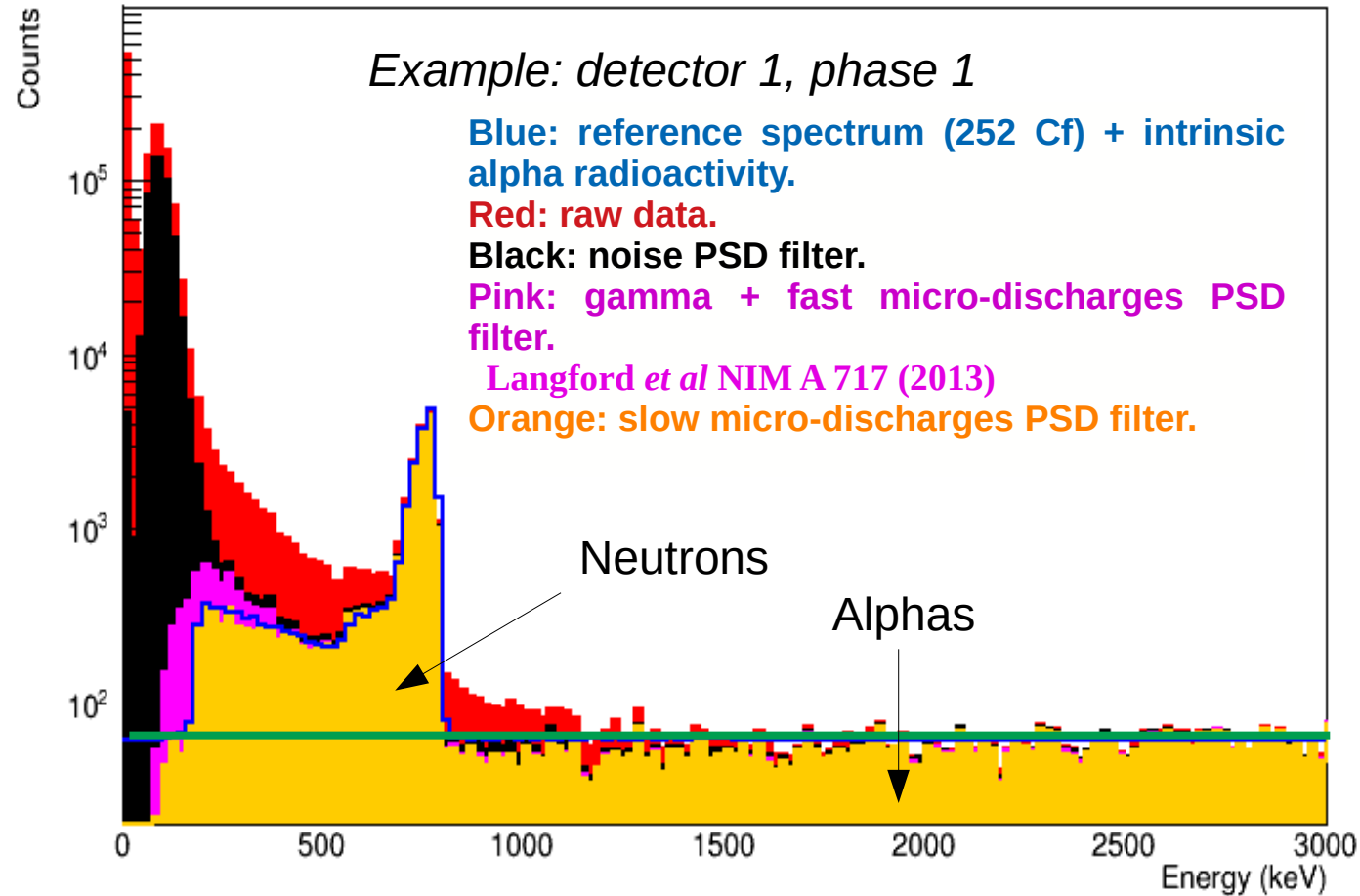
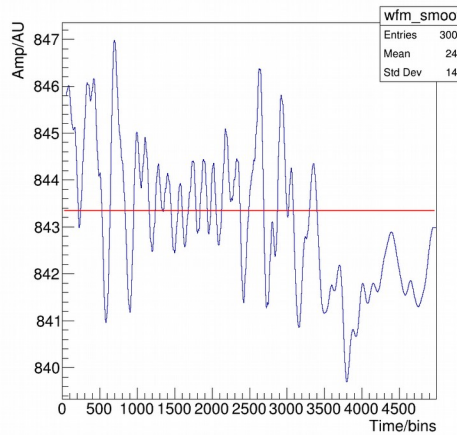


Neutron contribution: reference spectrum method



Neutron contribution: PSD

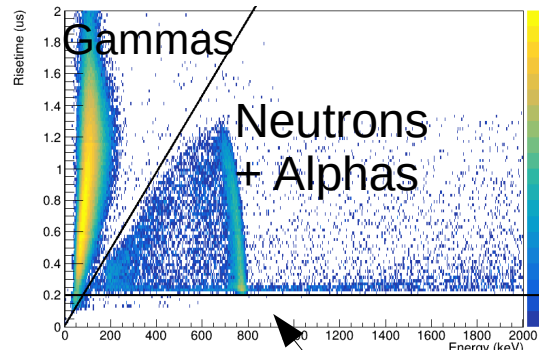
Black: noise PSD filter



Neutron contribution: PSD

Pink: gamma and fast micro-discharges PSD filter.

Langford et al NIM A 717 (2013)



Fast micro-discharges

Example: detector 1, phase 1

Blue: reference spectrum (^{252}Cf) + intrinsic alpha radioactivity.

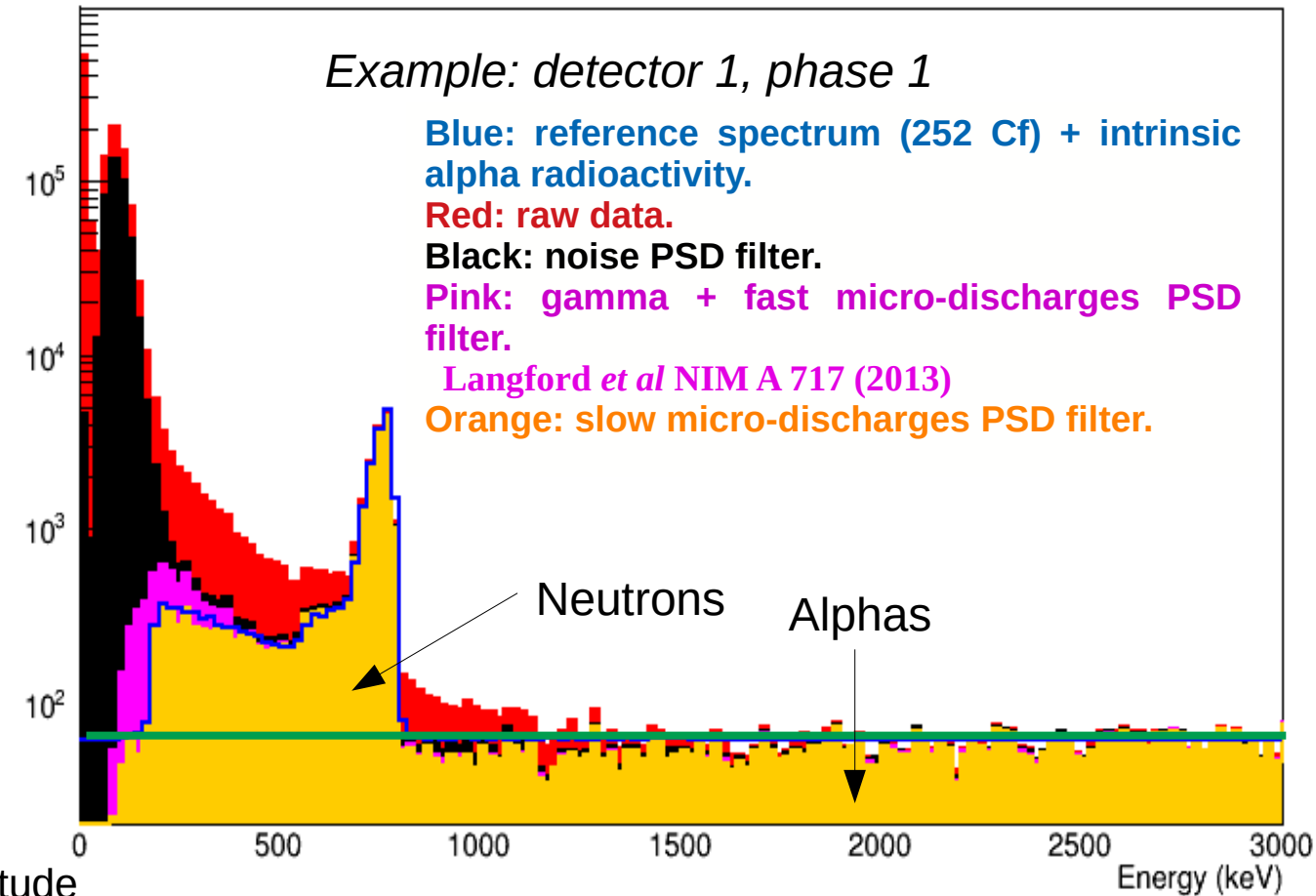
Red: raw data.

Black: noise PSD filter.

Pink: gamma + fast micro-discharges PSD filter.

Langford et al NIM A 717 (2013)

Orange: slow micro-discharges PSD filter.

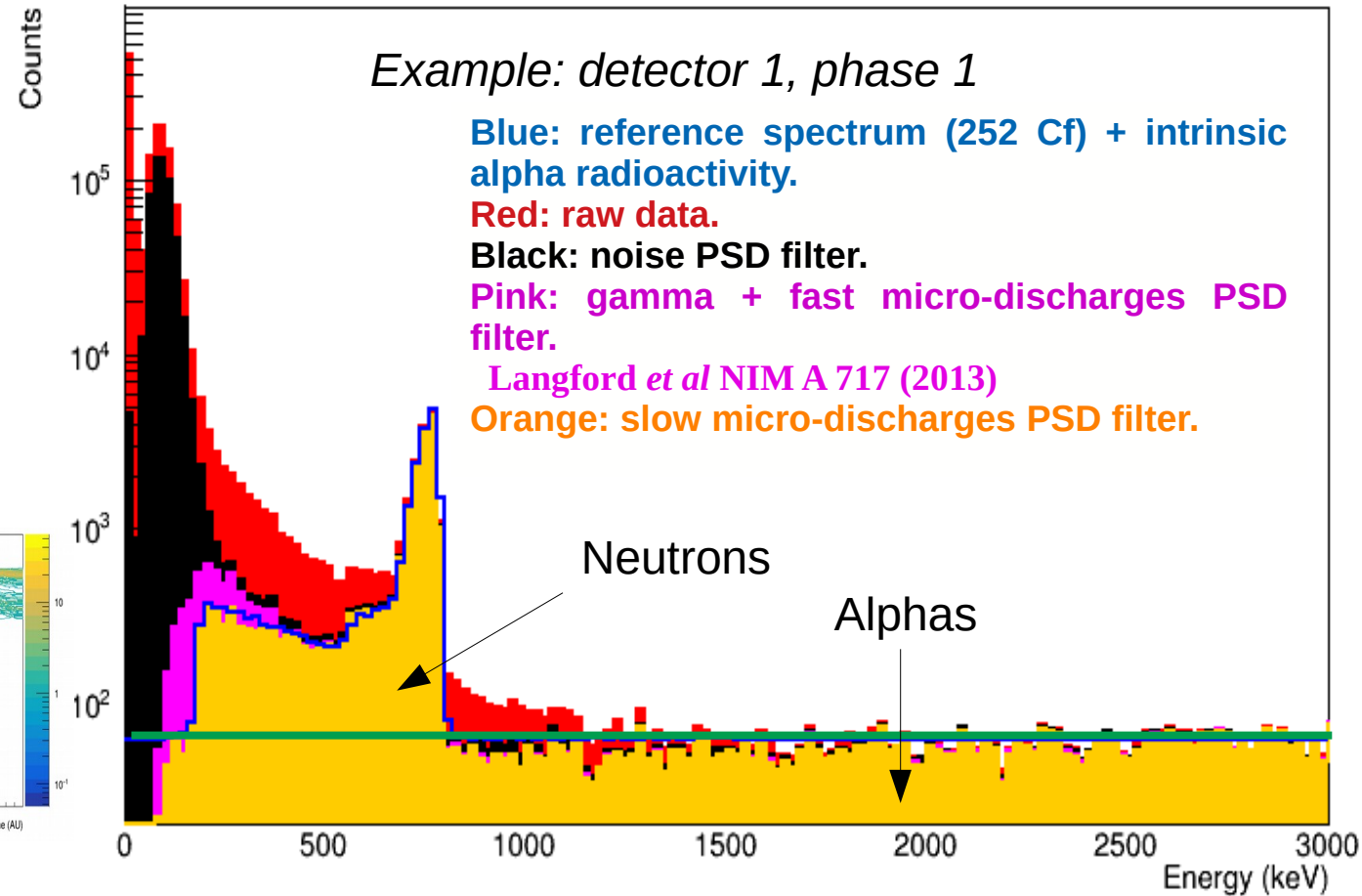
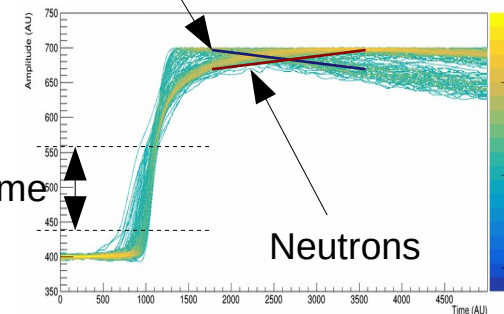


Risetime $\sim 10 - 50\%$ max. amplitude

Neutron contribution: PSD

Orange: micro-discharges PSD filter.

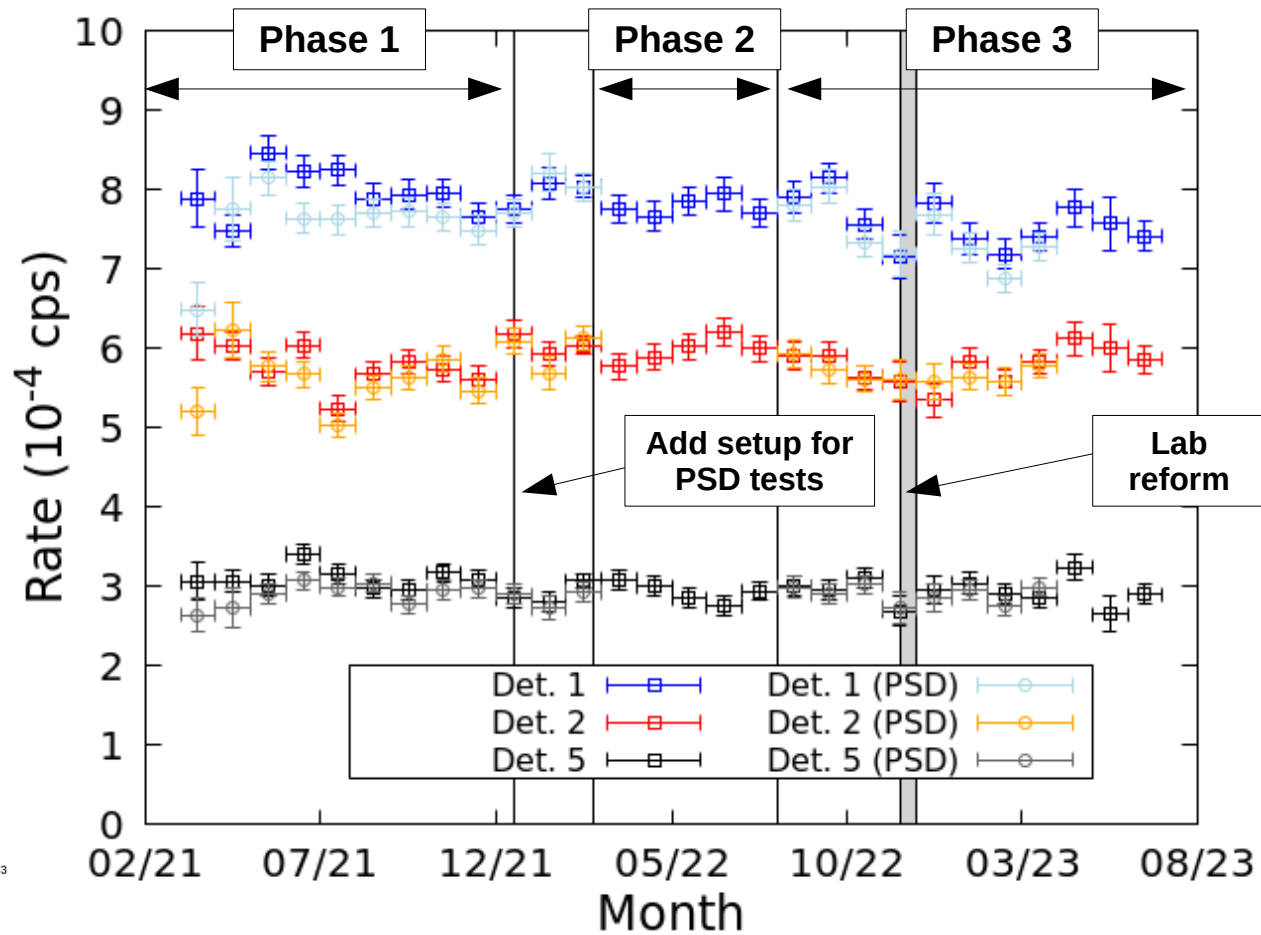
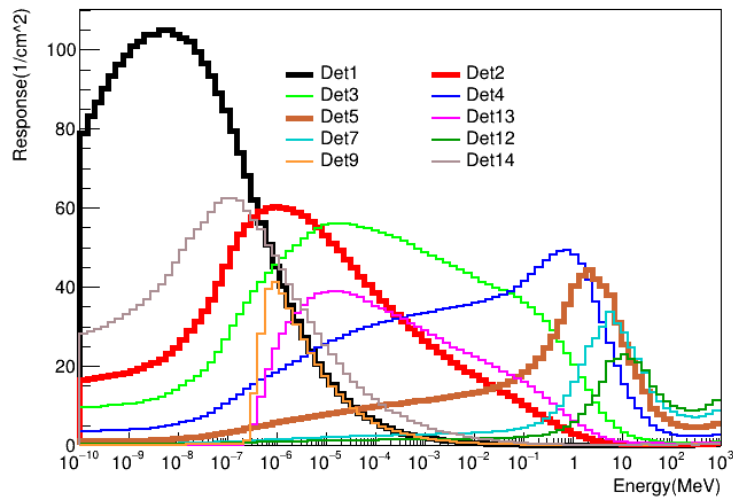
Slow micro-discharges



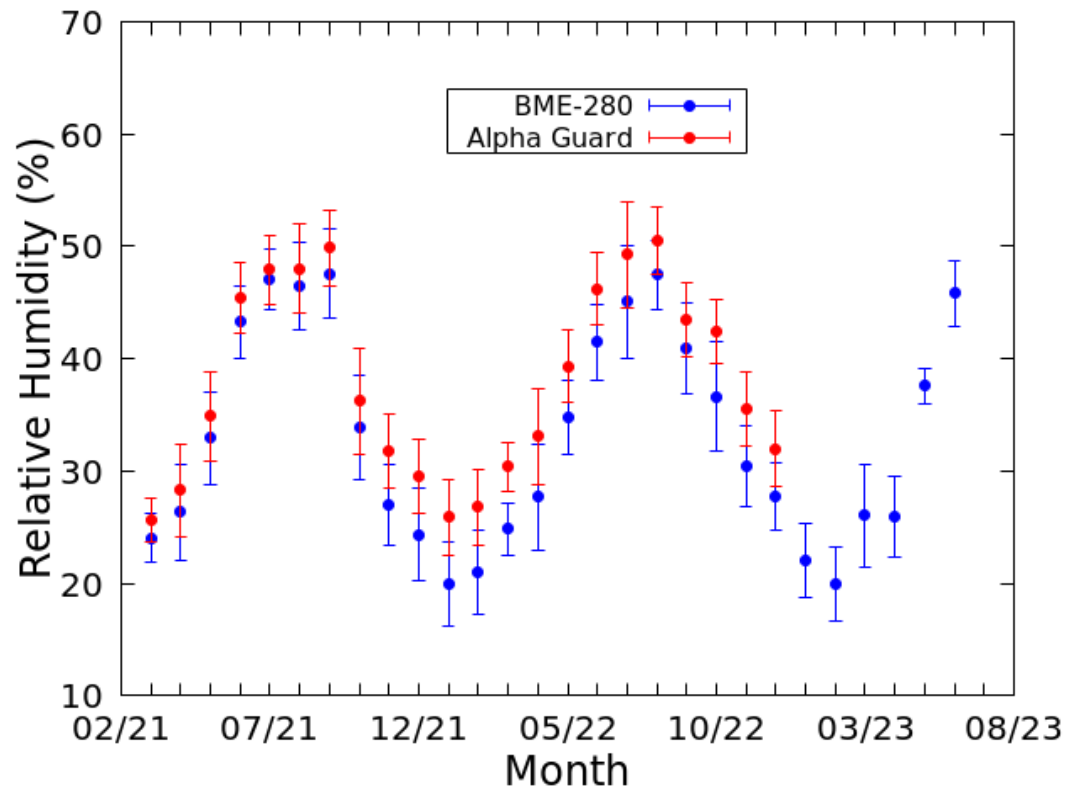
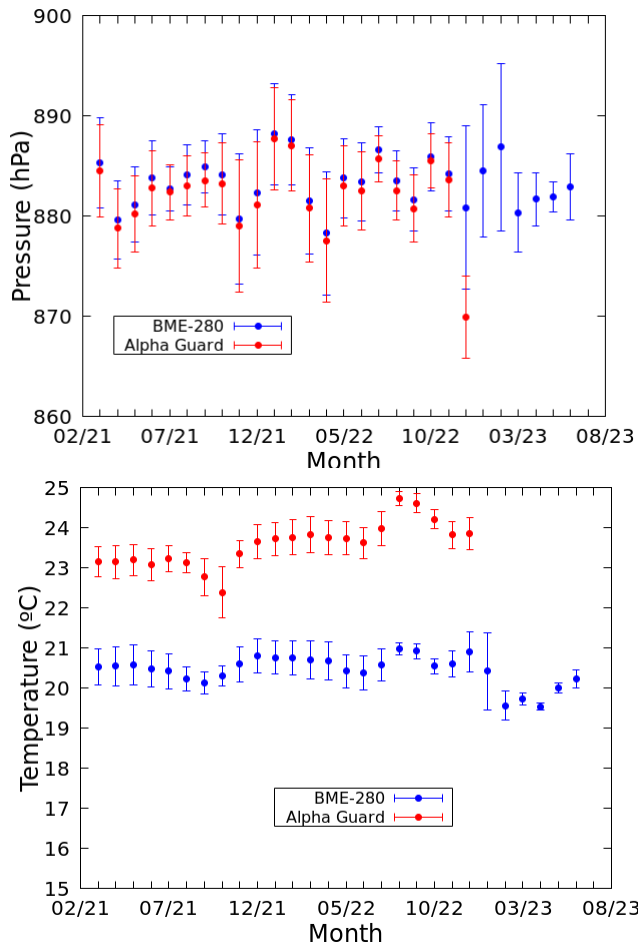
Monitoring the neutron flux in hall B

Counting rates (2 years)

Stable within the statistical margin of uncertainty.

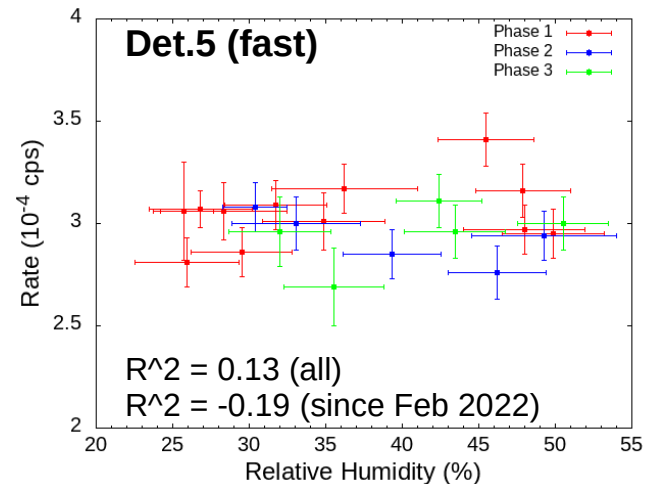
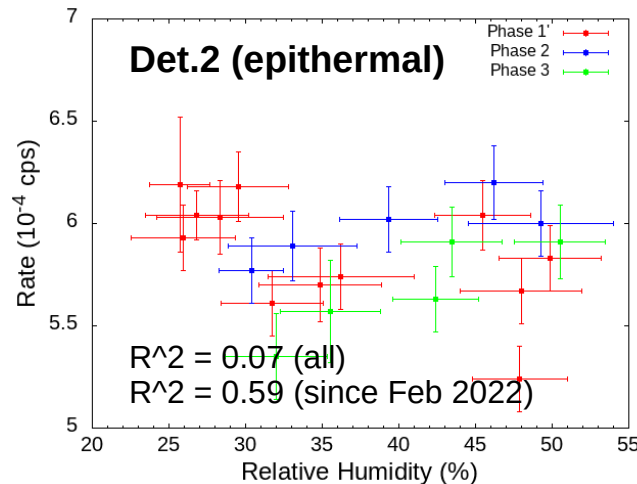
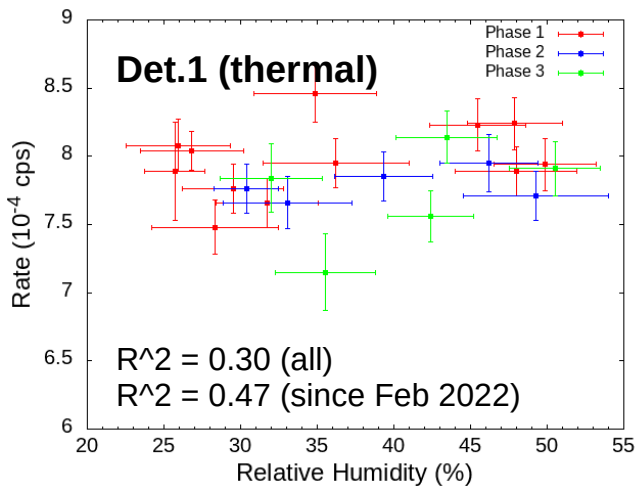


Environmental variables



RH proportional to mass H₂O in air
(T and P constant)

Correlations humidity – neutrons rates



Neutron energy distribution

Unfolding algorithms

- Bayesian method: **S. Agostini, NIM A 362 (1995) 487**
 - Computational implementation by J.L Tain (IFIC) and D. Cano-Ott (CIEMAT).
- GRAVEL and MAXED implemented in UMG package version 3.3 (free-distributed by PTB).
 - MAXED: **M. Reginatto et al., NIM A 476 (2002) 242**
 - GRAVEL: **M. Matzke, Report PTB-N-19 (1994)**

Unfolding results (preliminary)

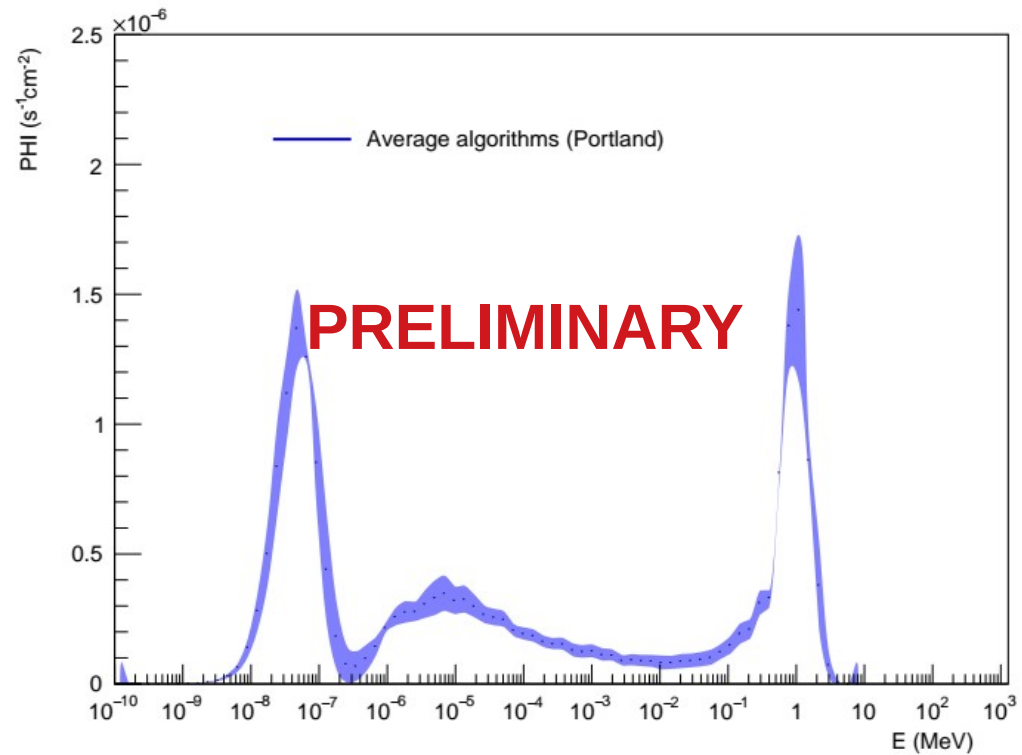
Setup version 2022 (rates: integral August – October 2022)

Average spectra with error-bands being the standard deviation.

Red: different algorithms, same prior.
Blue: same algorithms, different priors.

Flux units: 10^{-6} MeV cm $^{-2}$ s $^{-1}$

Region	Priors	Algorithms
Thermal	7.0(4)	7.3(4)
Intermediate	6.9(3)	6.8(2)
Fast	6.2(4)	6.0(4)
Total	20.1(6)	20.1(6)



Unfolding results (preliminary)

Setup version 2022 (rates: integral August – October 2022)

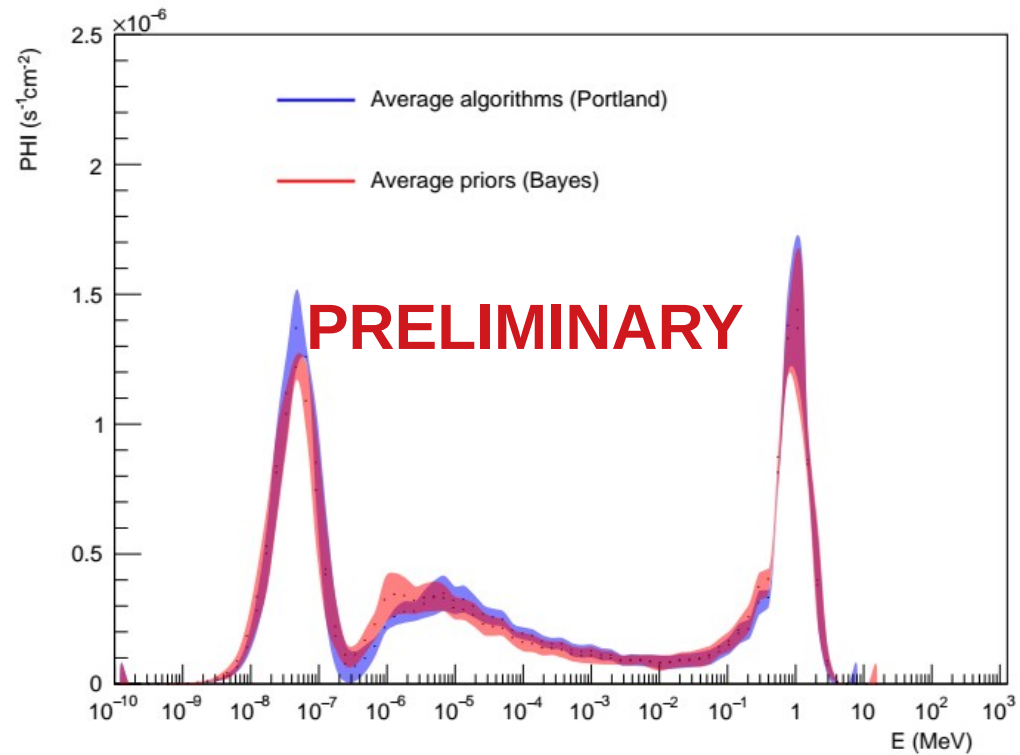
Average spectra with error-bands being the standard deviation.

Red: different algorithms, same prior.

Blue: same algorithms, different priors.

Flux units: 10^{-6} MeV cm $^{-2}$ s $^{-1}$

Region	Priors	Algorithms
Thermal	7.0(4)	7.3(4)
Intermediate	6.9(3)	6.8(2)
Fast	6.2(4)	6.0(4)
Total	20.1(6)	20.1(6)



Summary

- **Understanding the neutron sources.**
 - According to MC simulations **concrete is the dominant neutron source.**
 - Calculated spectra used as prior information in the unfolding algorithms.
- **Characterization of the temporal evolution of the neutron flux.**
 - Consistency using two different semi-independent data analysis methods.
 - The **counting rates are stable within the statistical uncertainties.**
 - Correlations between the counting rates and the air humidity have been studied.
- **Characterization of neutron flux energy spectrum.**
 - Since August 2022, an optimized setup is being used.
 - Different methods and priors converges to the same results.
 - Larger flux than in hall A.
 - Neutron flux in hall A: **$16.6(2) \cdot 10^{-6} \text{ cm}^{-2} \text{ s}^{-1}$** (S. Orrigo et al EPJ C 82, 2022)
 - **Preliminary** neutron flux in hall B: **$20.1(6) \cdot 10^{-6} \text{ cm}^{-2} \text{ s}^{-1}$**

Future work

- **Understanding the neutron sources.**
 - MC simulations: impact of the data libraries in the (α, n) production yields.
 - Study of the impact of the humidity.
 - Experimental characterization of the concrete, measurements without concrete
- **Characterization of the temporal evolution of the neutron flux.**
 - Data acquisition with full spectroscopic setup (10 det.) foreseen until 2025.
 - Set limits on the potential neutron flux modulation.
- **Characterization of neutron flux energy spectrum.**
 - To explore alternative techniques to determine the thermal and fast flux.
 - Improvement of the response calculations.

List of authors

Institute of Energy Technologies - Technical University of Catalonia (INTE – UPC)

N. Mont-Geli, G. Cortés, M. Pallàs, F. Calviño, A. De Blas, R. Garcia



UNIVERSITAT POLITÈCNICA DE CATALUNYA
BARCELONATECH

Institut de Tècniques Energètiques

Instituto de Física Corpuscular (IFIC, CSIC – UV)

A. Tarifeño-Saldivia, S.E.A. Orrigo, J.L. Tain, E. Nacher, J. Agramunt, A. Algora



University of Granada

A. Quero-Ballesteros, A. Lallena



UNIVERSIDAD
DE GRANADA



UNIVERSIDAD
COMPLUTENSE
MADRID

Universidad Complutense de Madrid (UCM)

L.M. Fraile

Helmholtz-Zentrum Dresden-Rossendorf (HZDR)

D. Bemmerer, M. Grieger

TRIUMF
I. Dillman



HZDR

HELMHOLTZ ZENTRUM
DRESDEN ROSSENDORF

Centro de Astropartículas y Física de Altas Energías – University of Zaragoza (CAPA) (ANAIS team)

J. Amaré, S. Cebrián, D. Cintas, I. Coarasa, E. García, M. Martínez, Y. Ortigoza, A. Ortiz de Solórzano, J. Puimedón, T. Pardo, M.L. Sarsa

CIEMAT
D. Cano-Ott, T. Martínez, J. Plaza



CAPA

Centro de Astropartículas y
Física de Altas Energías
Universidad Zaragoza

Acknowledgements

This work was supported by the Spanish MICINN Grants No. PID2019-104714GB-C21, PID2019-104714GB-C22, FPA2017-83946-C2-1-P and FPA2017-83946-C2-2-P (MCIU/AEI/FEDER).

We acknowledge the support of the Generalitat Valenciana Grant No. PROMETEO/2019/007.

L.M.F. acknowledges support from the project No. RTI2018-098868-B-I00.

We are grateful to Laboratorio Subterráneo de Canfranc for hosting the HENSA spectrometer, for the support received by the LSC personnel during the measurement campaign.

Backup slides

The High Efficiency Neutron Spectrometry Array



HENSA experimental setup

- Ten neutron detectors.
 - **60 cm active length cylindrical ${}^3\text{He}$ -filled neutron proportional counters** manufactured by LND (in general, 10 atm gas pressure).
 - Moderators (HDPE, Cd, Pb) with different sizes in order to provide sensitivity in different regions of the neutron flux spectrum (**non-spherical geometries**).
- Electronics:
 - Preamplifiers (CAEN, Canberra, Fast).
 - High Voltage supply (CAEN).
- Data acquisition using a SIS3316 struck digitizer + Gasific software (list mode)

Monte Carlo simulations of the neutron flux

Three neutron sources are considered

- Muon-induced neutrons.
 - Muon transport, neutron production and neutron transport calculated using FLUKA.
- (α,n) reactions.
 - Neutron transport calculated using FLUKA, neutron production calculated using specialized codes.
- Spontaneous fission (SF).
 - Neutrons transport using FLUKA, neutron production from experimental measurements.

For the (α,n) reactions and the SF calculations are carried out separately for the neutron production in the mountain rock and in the concrete walls of the laboratory.

Humidity effects not considered.

Based in the work by M. Grieger (HZDR) at Felsenkeller:
M. Grieger et al 2020, Phys. Rev. D 101, 123027

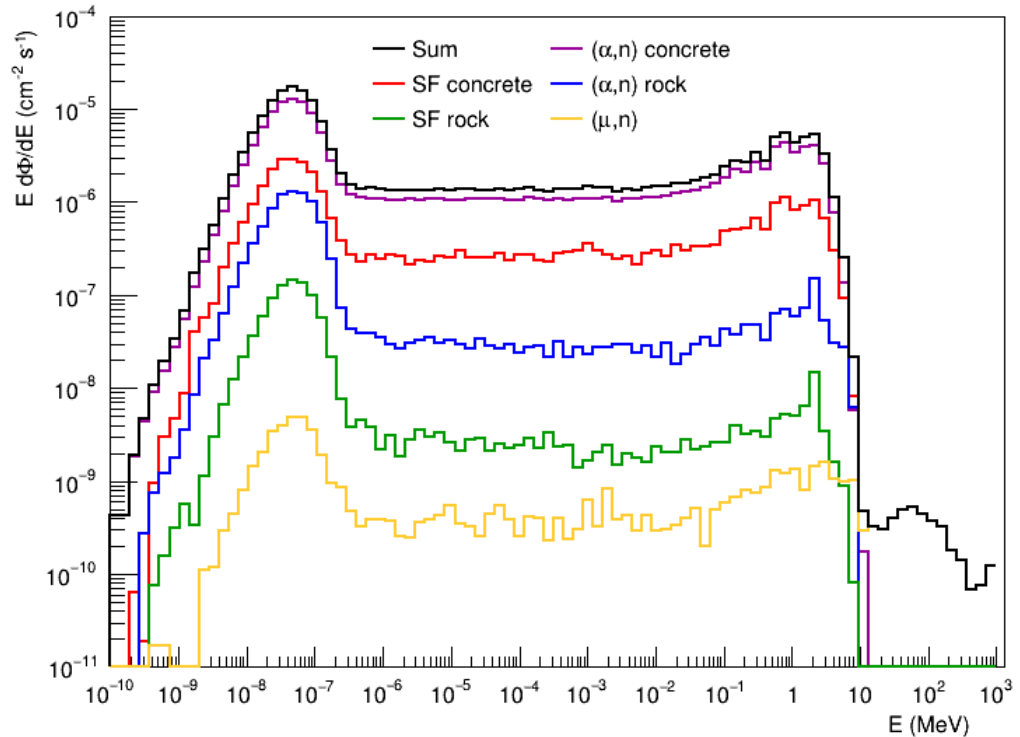
Monte Carlo simulations of the neutron flux

Example: Portland concrete

Integral fluxes (units $10^{-6} \text{ cm}^{-2} \text{ s}^{-1}$) at the measurement location (hall A):

- (α,n) reactions in the rock: 3.19(3).
- (α,n) reactions in the concrete: 53.66(4).
- Spontaneous fission in the rock: 0.550(6).
- Spontaneous fission in the concrete: 12.48(11).
- Muon-induced neutrons: 0.0207(5)**.
- Sum of all contributions: 69.90(12).
- Concrete contribution [$(\alpha,n) + \text{SF}$] 66.14(12).

**Preliminary estimation.



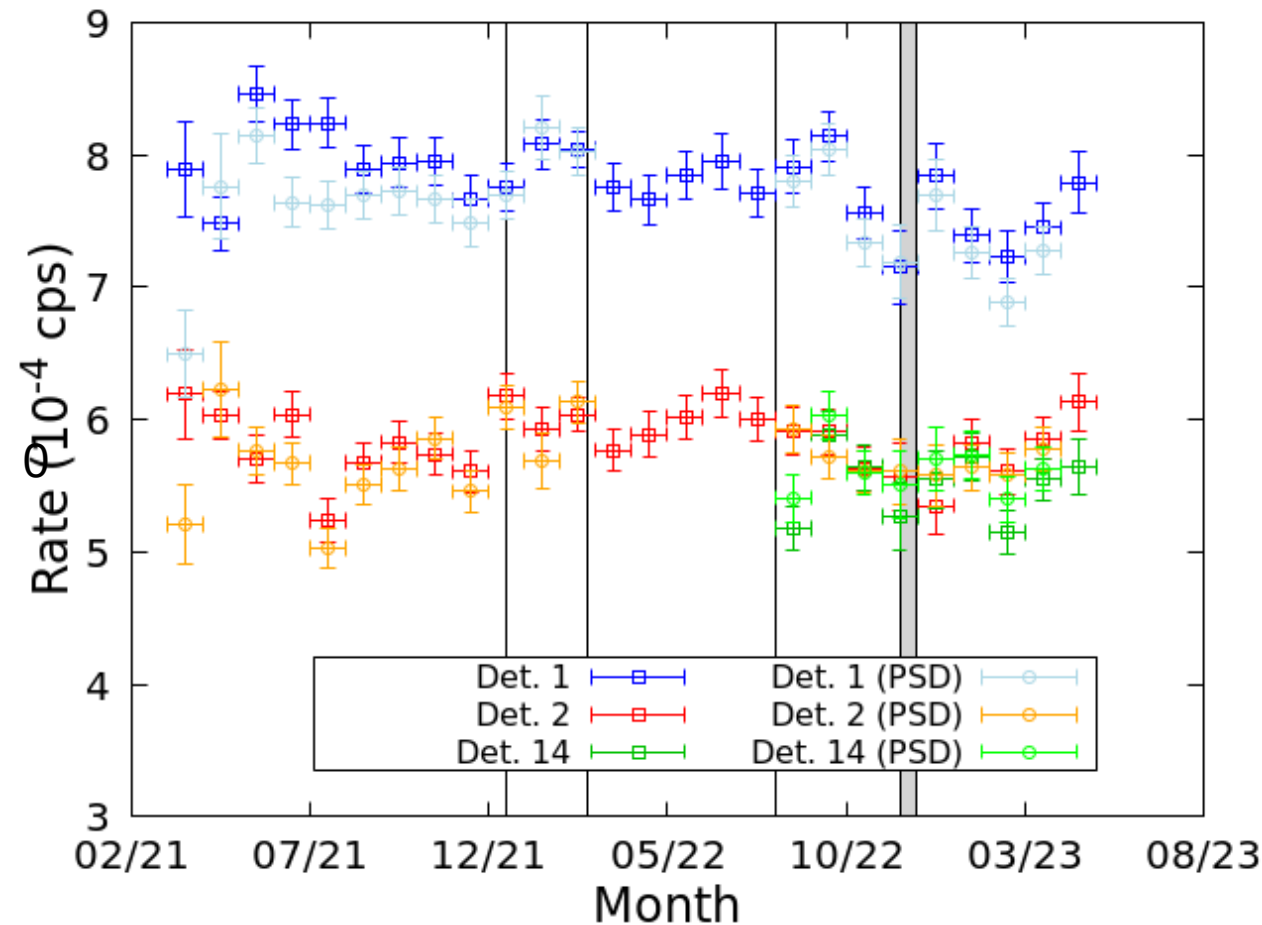
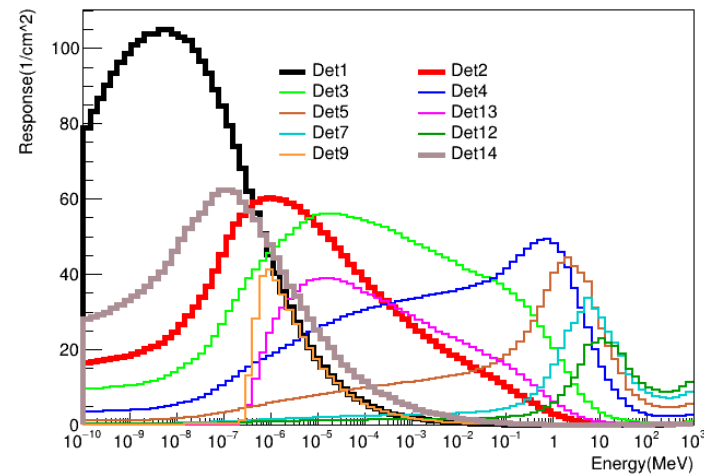
Based in the work by M. Grieger at Felsenkeller:

M. Grieger et al 2020, Phys. Rev. D 101, 123027

Data analysis: counting rates

Counting rates (low energy)

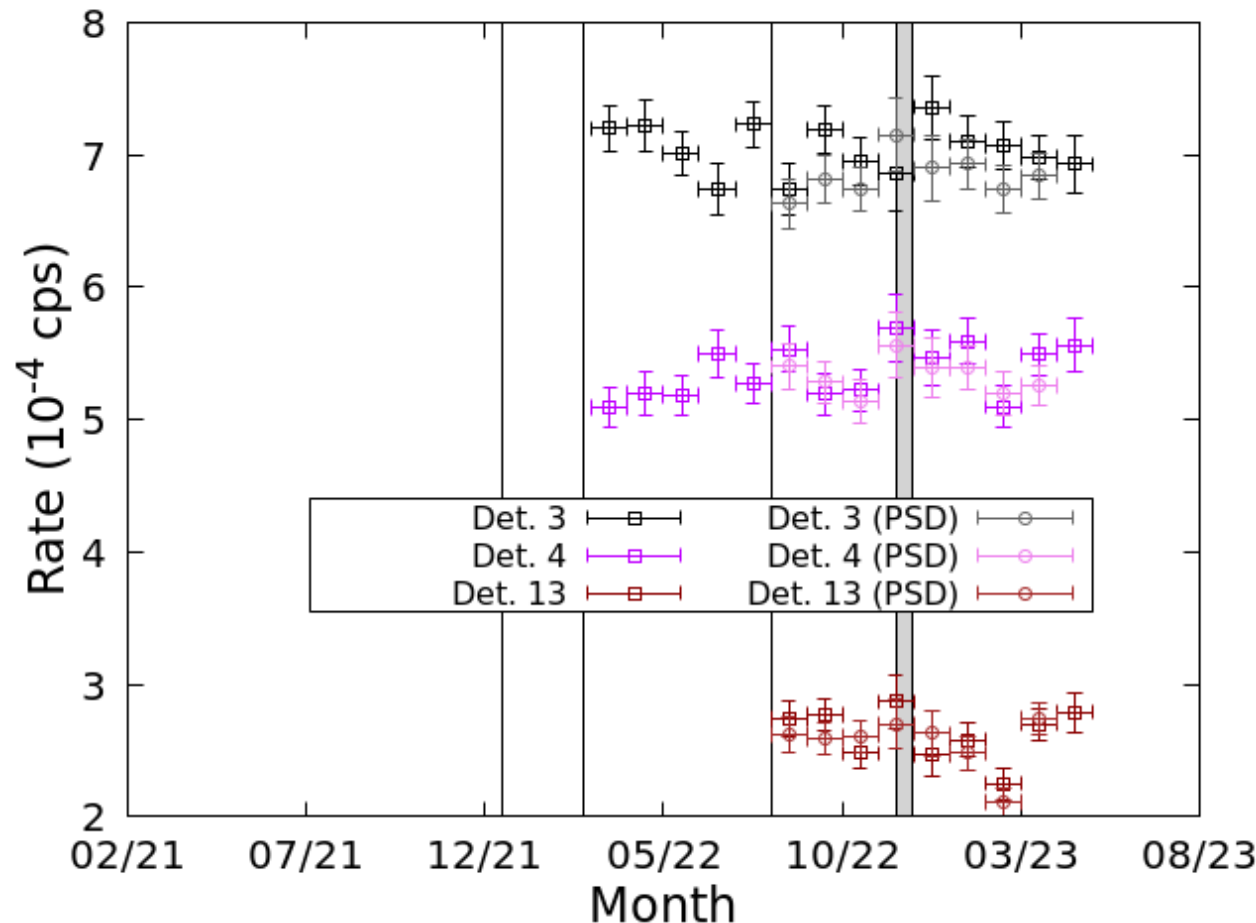
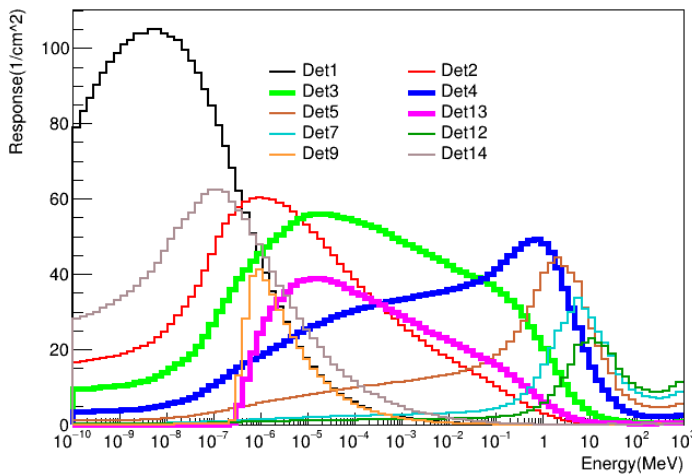
Stable within the statistical margin of uncertainty.



Data analysis: counting rates

Counting rates (intermediate energy)

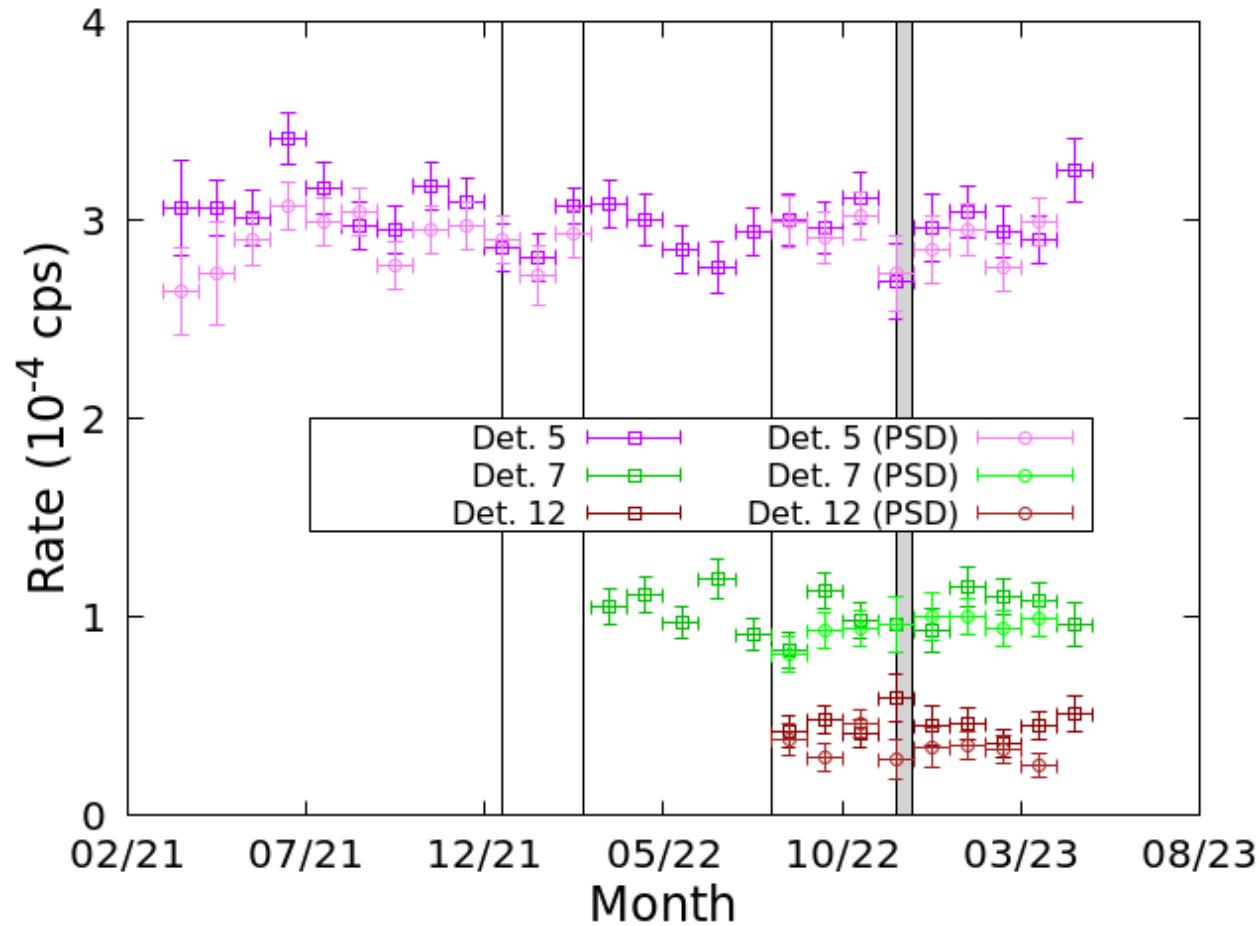
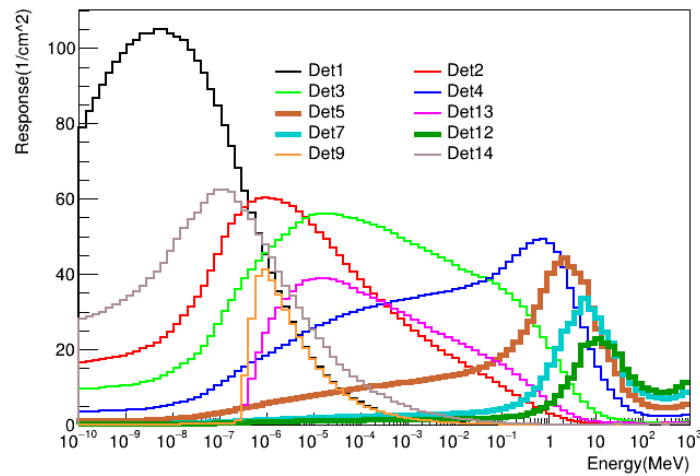
Stable within the statistical margin of uncertainty.



Data analysis: counting rates

Counting rates (fast energy)

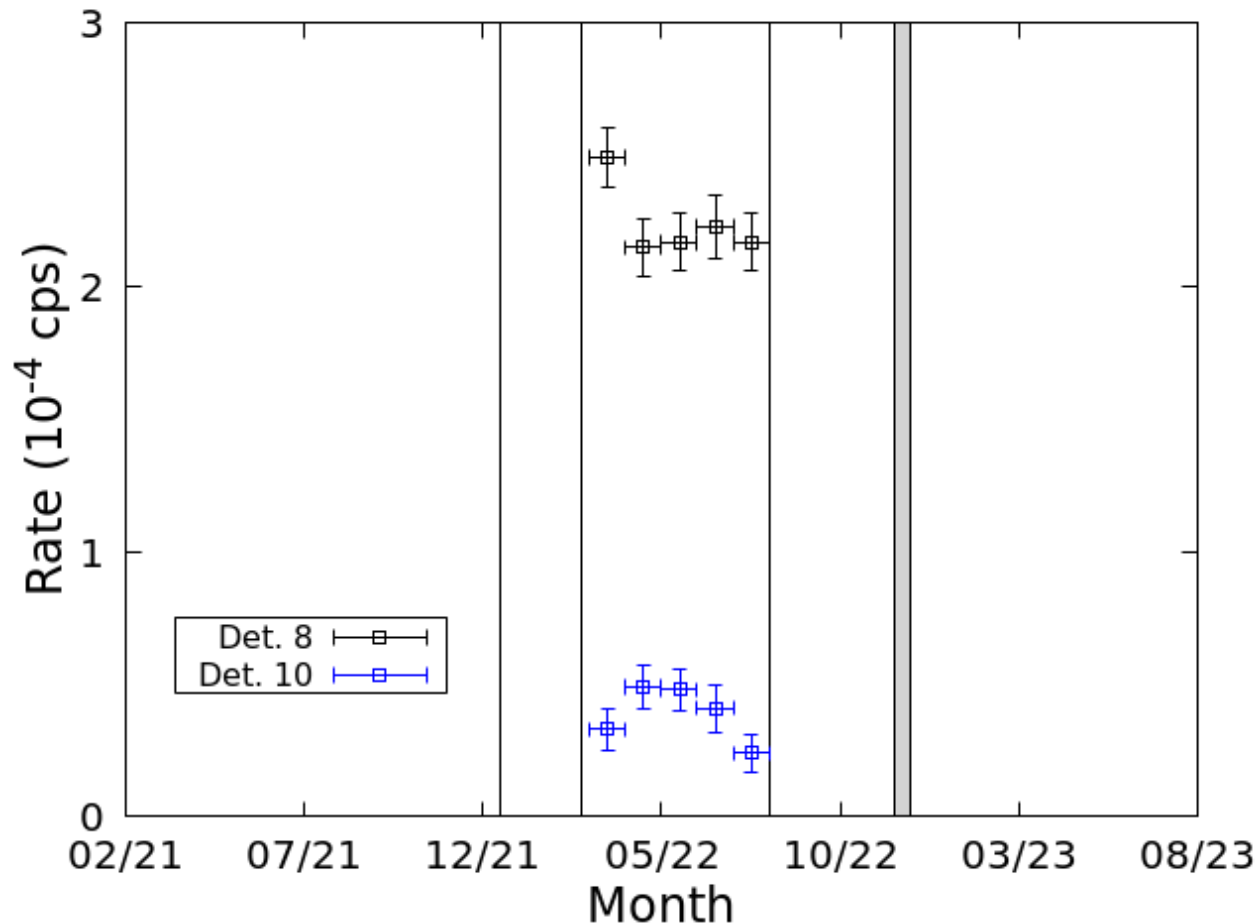
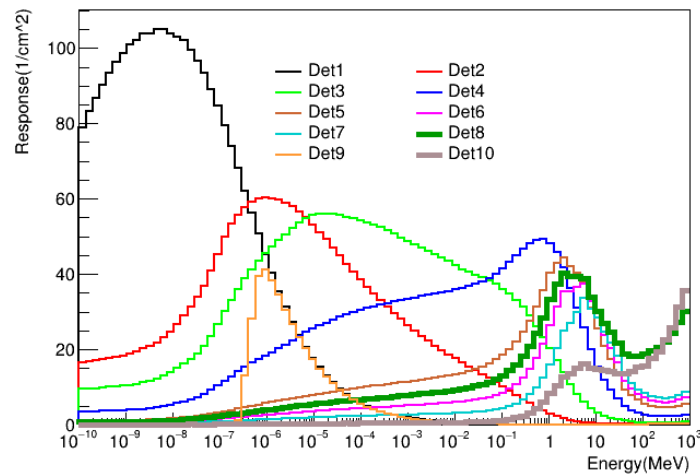
Stable within the statistical margin of uncertainty.



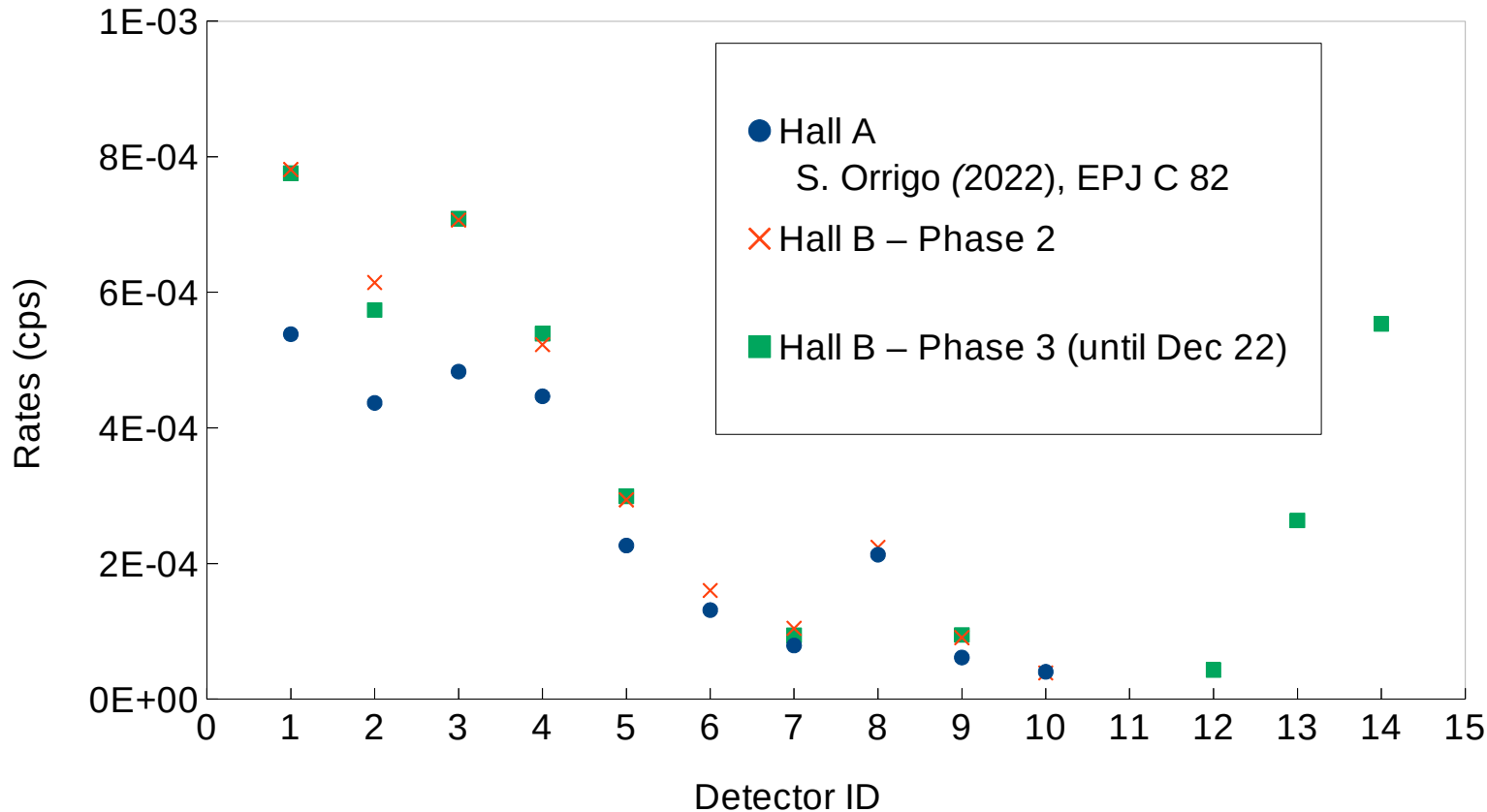
Data analysis: counting rates

Counting rates (HE energy)

Stable within the statistical margin of uncertainty.

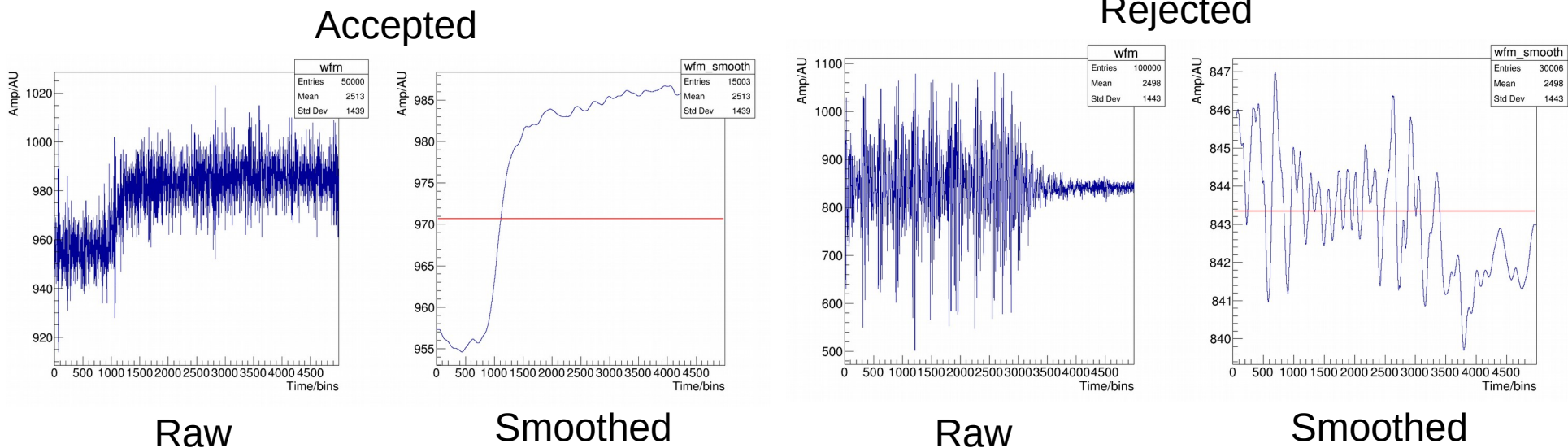


Average rates



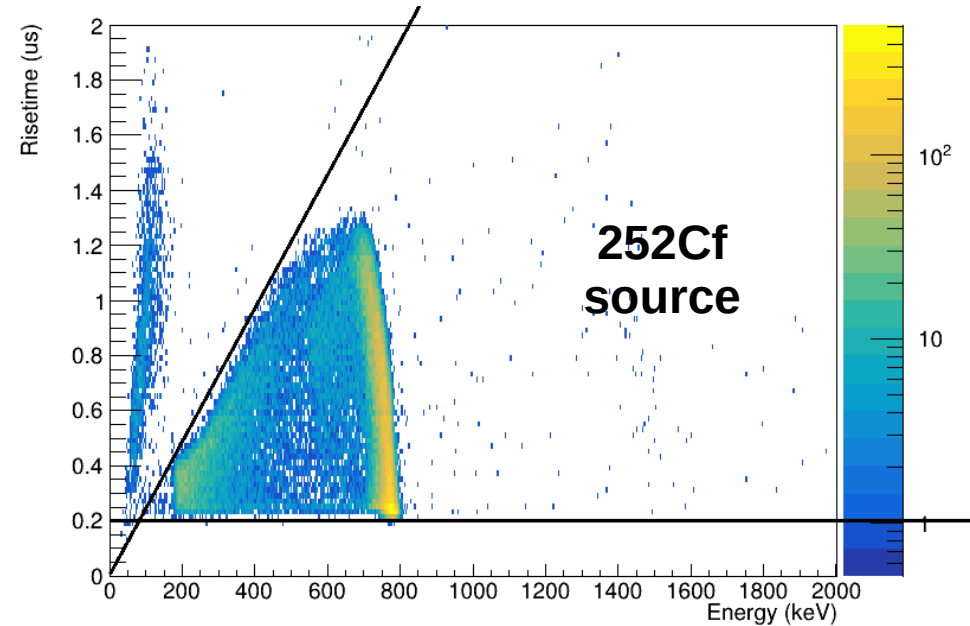
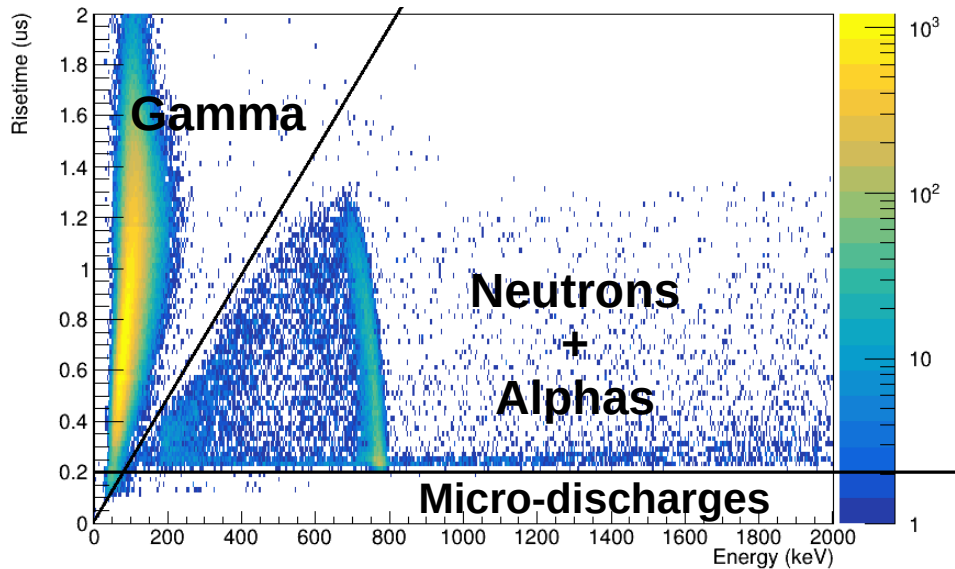
PSD: noise “filter”

A filter based on the oscillatory shape of the noise signals.



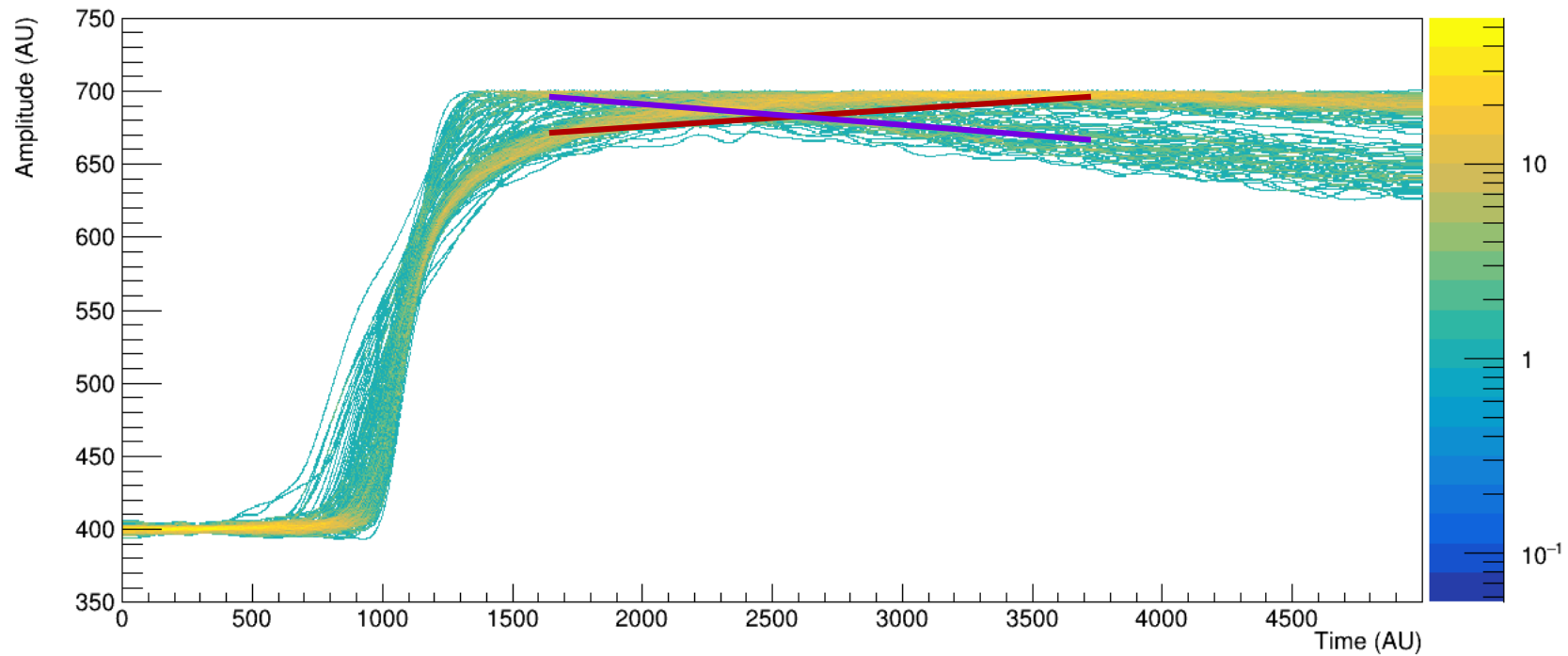
PSD: gamma-neutron discrimination

A filter based on the risetime differences: Langford *et al* NIM A 717 (2013)



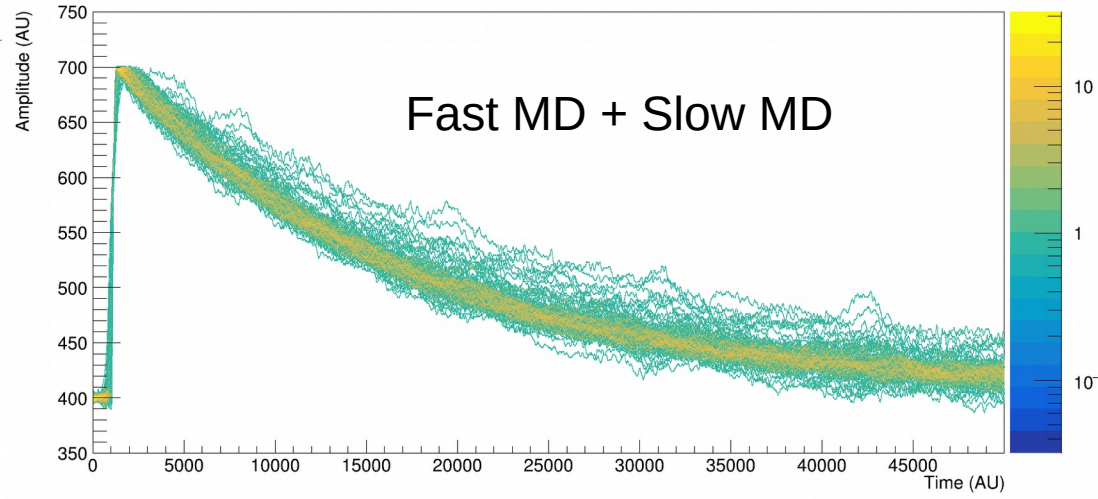
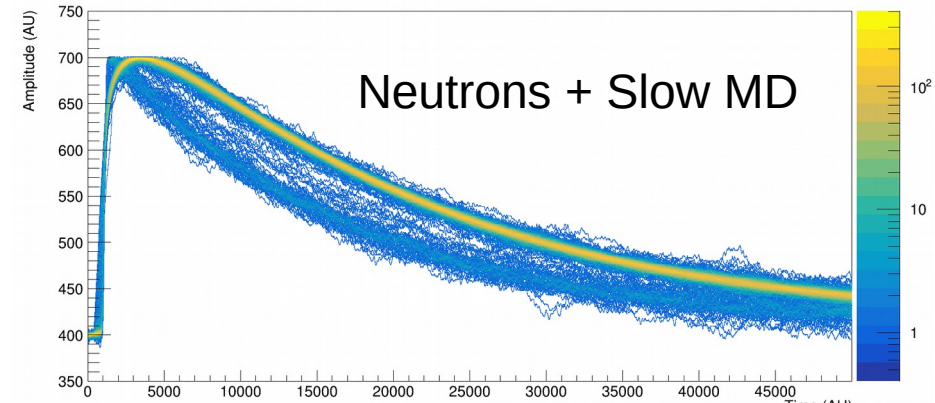
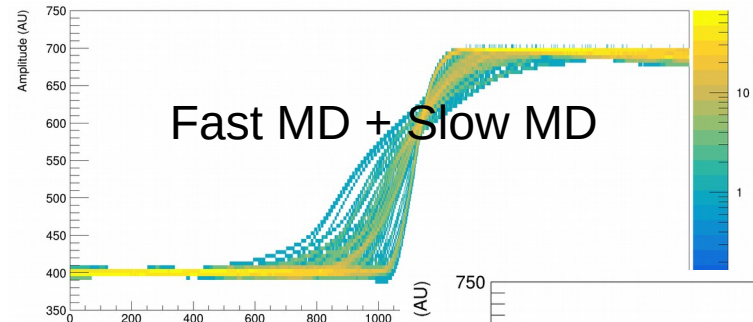
PSD: slow micro-discharges “filter”

A filter based on the decay shape.



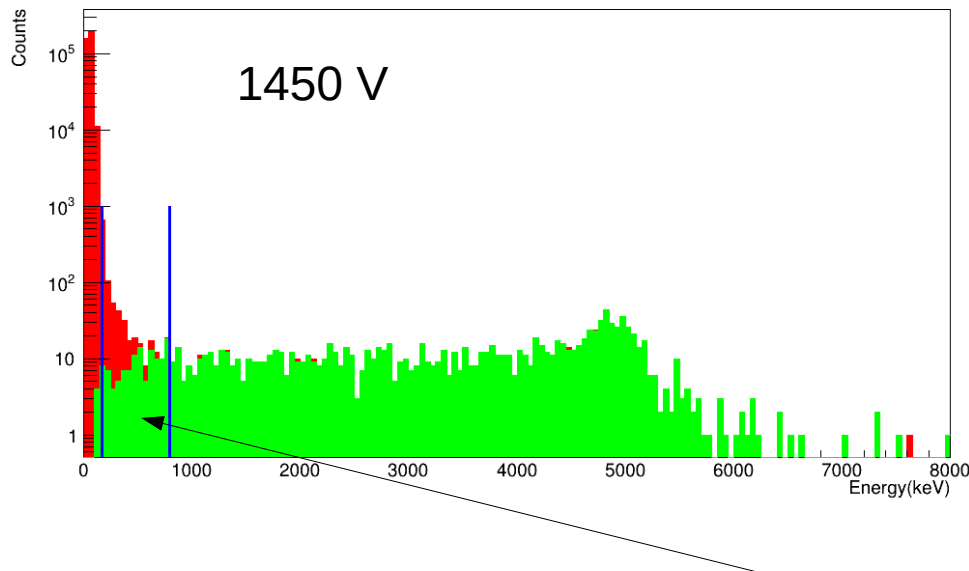
PSD: slow and fast micro-discharges

Different risetime, same decay

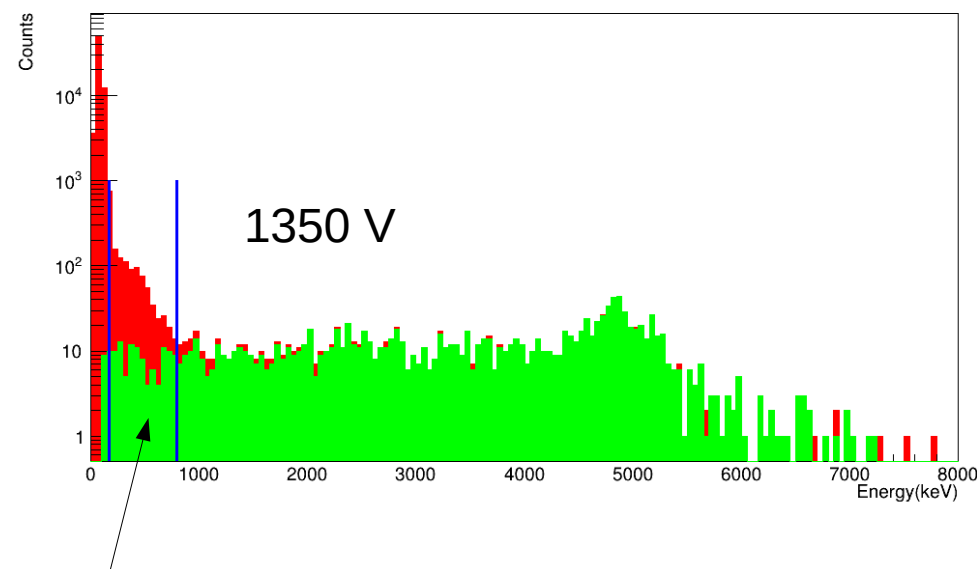


Validation of the alpha background hypothesis

Setup: thermal neutrons counter (T) + Cd (thermal shielding) + HDPE



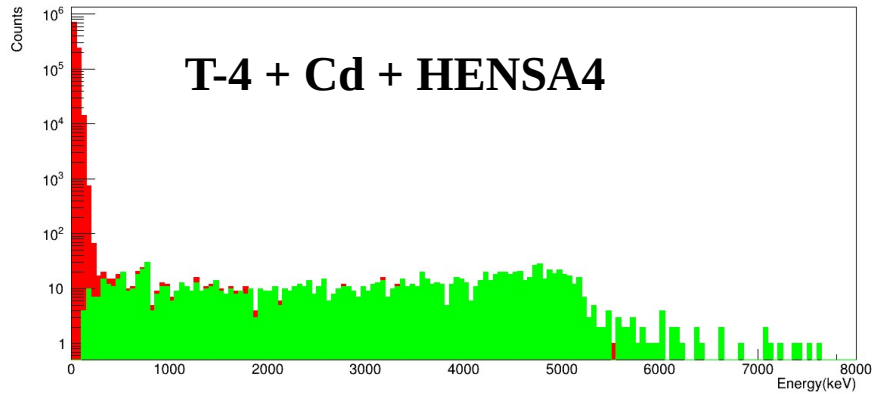
1450 V



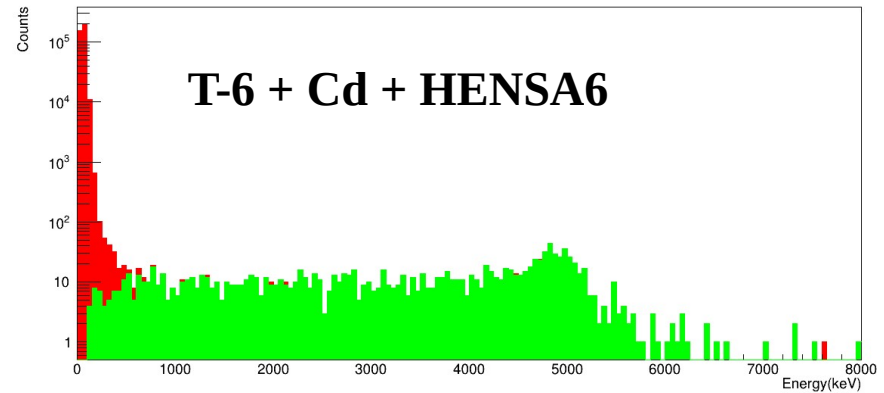
1350 V

Neutron window (170 – 800 keV)

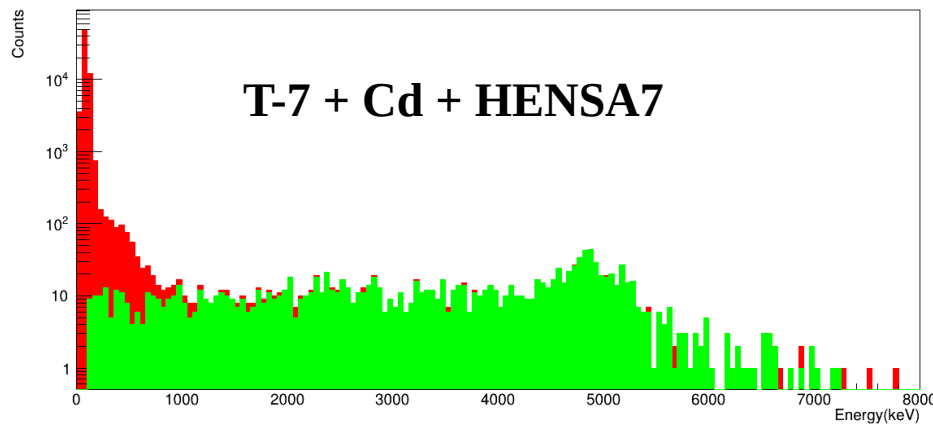
Alpha background



T-4 + Cd + HENSA4

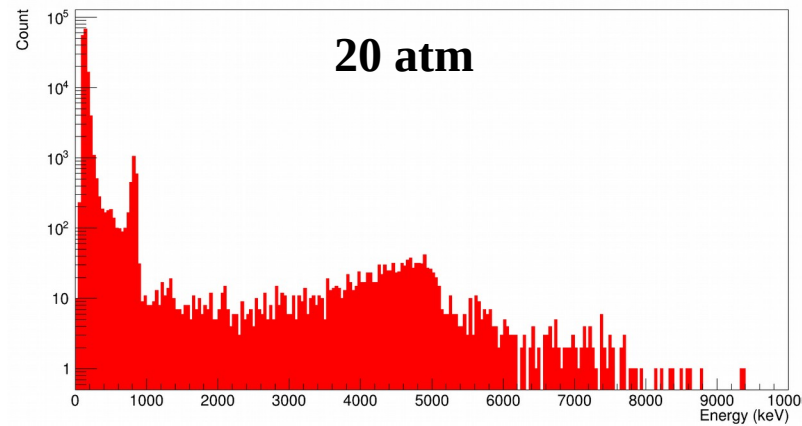
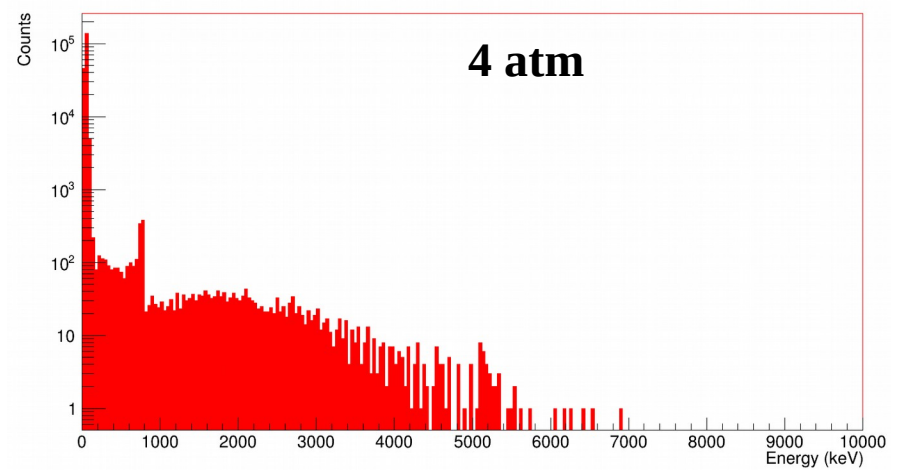
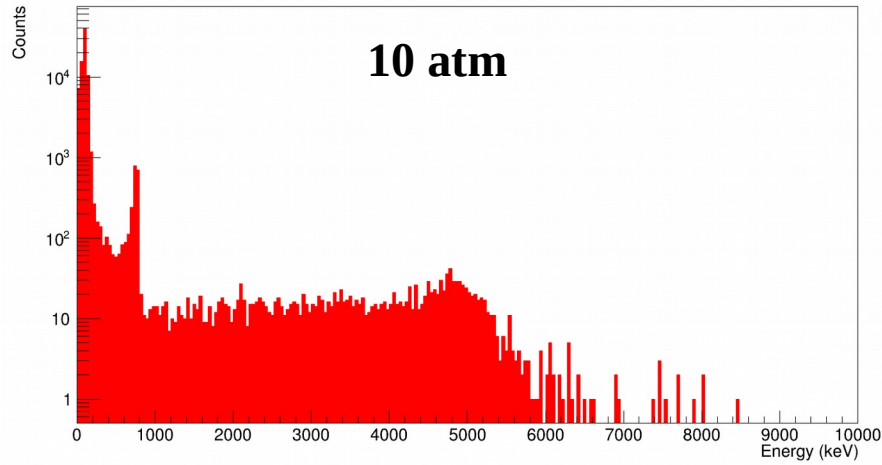


T-6 + Cd + HENSA6



T-7 + Cd + HENSA7

Alpha background



Data analysis: unfolding (HE peak)

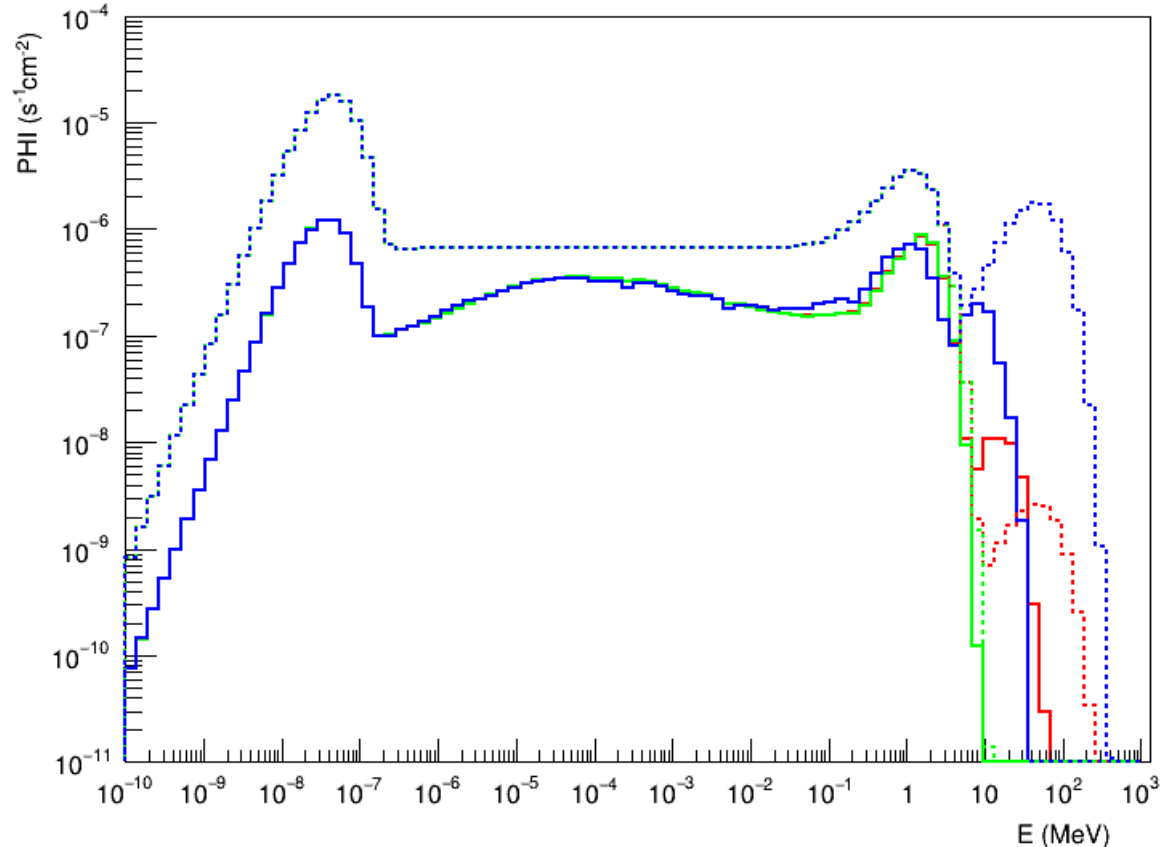
Setup version 2019

“Synthetic” priors.

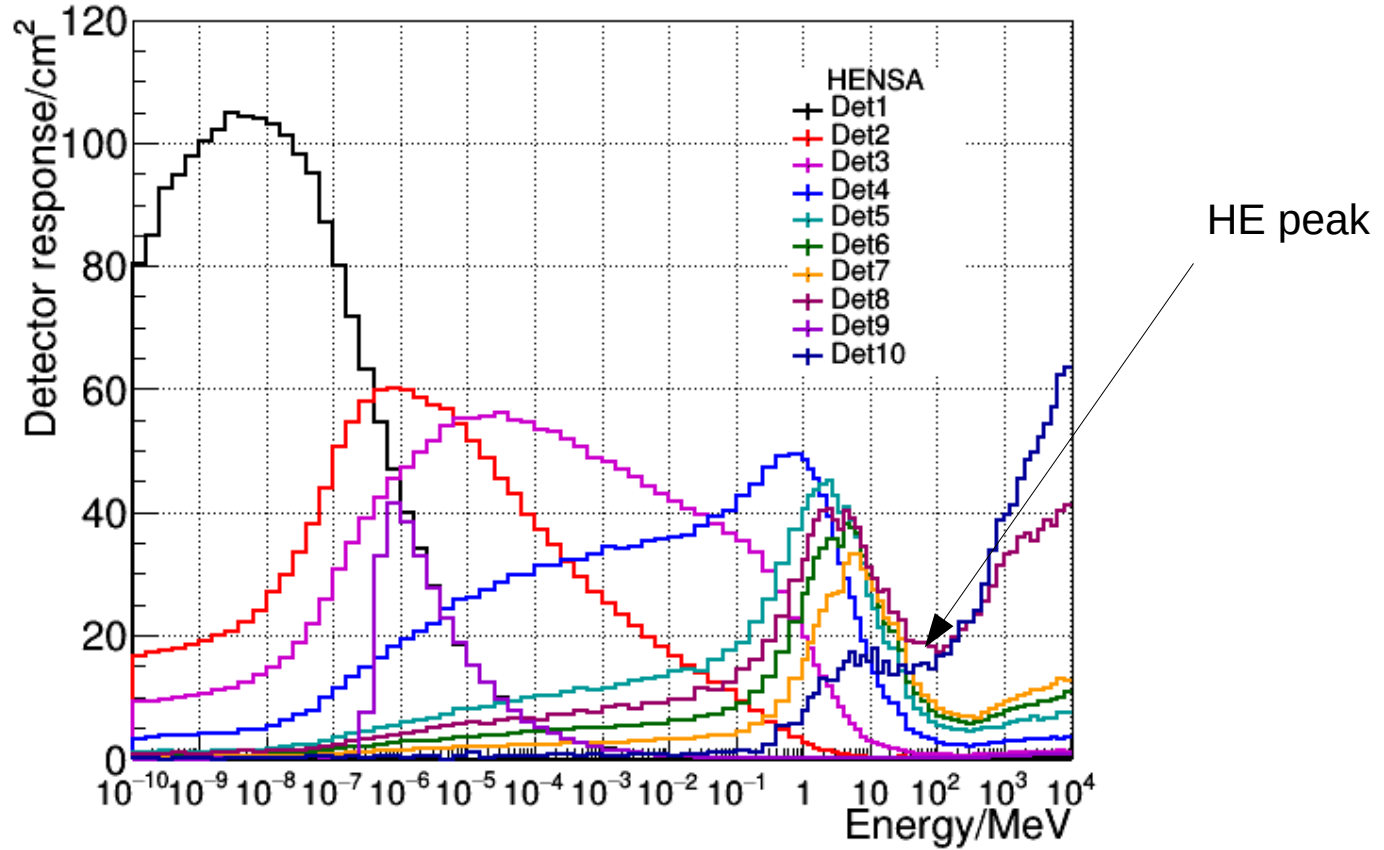
Test the **energy resolution** capabilities
in the **high energy region**.

Prior-dependent results.

Bayes algorithm.



Data analysis: unfolding (HE peak)



Data analysis: unfolding (fast peak position)

Setup version 2019

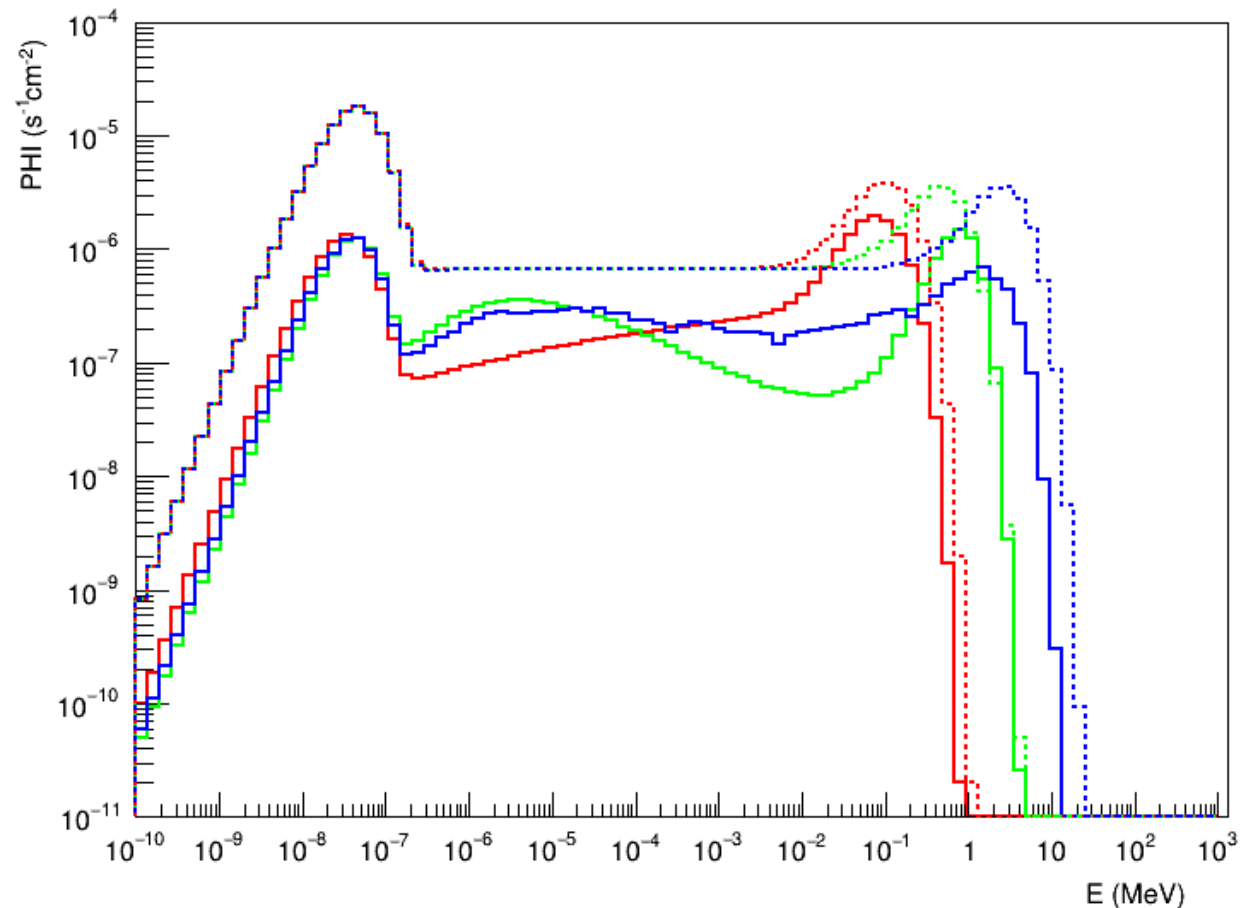
“Synthetic” priors.

Test the **energy resolution** capabilities
in the **fast region**.

Prior-dependent results.

*Unfolding not possible with the red prior.

Bayes algorithm.



Data analysis: unfolding (fast peak position)

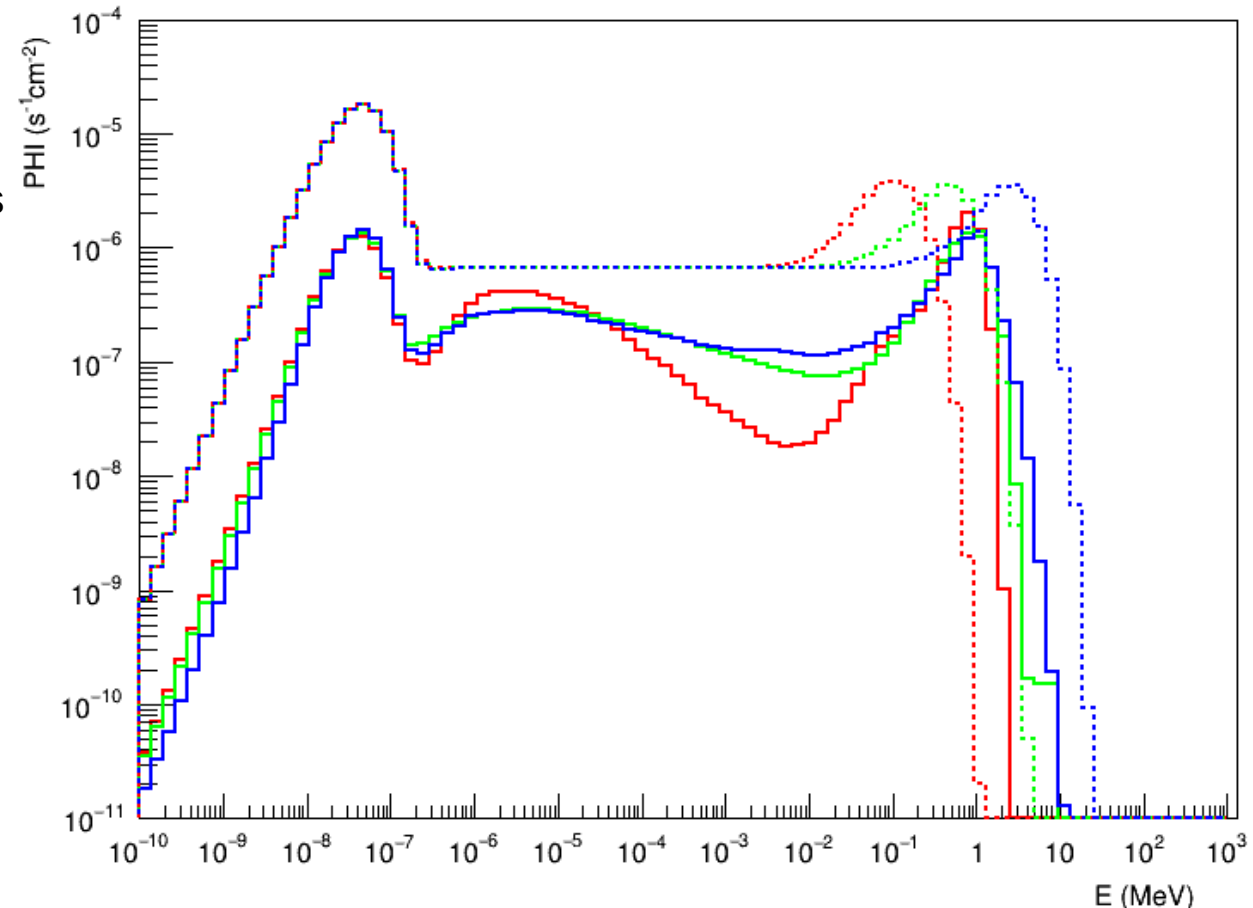
Setup version 2022

“Synthetic” priors.

Test the **energy resolution** capabilities
in the **fast region**.

All priors converges (in the fast region).

Bayes algorithm.



Integral flux

Thermal flux ($E < 3.2 \cdot 10^{-7}$ MeV)

Intermediate flux ($3.2 \cdot 10^{-7}$ MeV $< E < 0.1$ MeV)

Fast flux (0.1 MeV $< E < 20$ MeV)

(Rates August – October 22)

- **Units: 10^{-6} MeV cm $^{-2}$ s $^{-1}$**

	Portland	Lim. Steel	Port. Iron	Port. Baryte	St. D. / Av.
Thermal	7.34(2)	7.11(2)	7.01(2)	6.87(2)	2%
Intermediate	6.74(1)	6.82(1)	6.84(1)	6.82(1)	1%
Fast	6.04(4)	6.16(3)	6.23(3)	6.35(3)	1.2%

Integral flux (Ph31)

Thermal flux ($E < 3.2 \cdot 10^{-7}$ MeV)

Intermediate flux ($3.2 \cdot 10^{-7}$ MeV $< E < 0.1$ MeV)

Fast flux (0.1 MeV $< E < 20$ MeV)

(Rates August – October 22)

* No errors analysis

- Units: 10^{-6} MeV cm $^{-2}$ s $^{-1}$

Portland	Bayes	MAXED	GRAVEL	St. D. / Av.
Thermal	7.34(2)	7.25*	7.35*	0.75%
Intermediate	6.74(1)	6.83*	6.73*	0.77%
Fast	6.04(4)	6.07*	6.05*	0.33%

Thermal flux

Thermal flux ($E < 3.2 \cdot 10^{-7}$ MeV)

- CIEMAT method: J. Plaza et al., Astroparticle Physics 146 (2023) 102793

$$R^{bare} = S_{th}^{bare} \Phi_{th} + S_{e+f}^{bare} \Phi_{e+f}$$
$$R^{Cd} = S_{th}^{Cd} \Phi_{th} + S_{e+f}^{Cd} \Phi_{e+f}$$

Units: 10^{-6} MeV cm $^{-2}$ s $^{-1}$

	Lim. Steel	Portland
Bayes unfolding	7.07(2)	7.28(2)
CIEMAT (no uncertainty estimation)	7.47	7.14

Neutron flux modulation in underground facilities

ISSN 1063-7796, Physics of Particles and Nuclei, 2017, Vol. 48, No. 1, pp. 34–37. © Pleiades Publishing, Ltd., 2017.

The Study of the Thermal Neutron Flux in the Deep Underground Laboratory DULB-4900^{1,2}

V. V. Alekseenko^a, Yu. M. Gavril'yuk^a, A. M. Gangapshev^{a, *}, A. M. Gezhaev^a,
D. D. Dzhappuev^a, V. V. Kazalov^a, A. U. Kudzhaev^a, V. V. Kuzminov^a, S. I. Panas^a,
S. S. Ratkevich^b, D. A. Tekueva^a, and S. P. Yakimenko^a

^aInstitute for Nuclear Research, RAS, Moscow, Russia

^bKharkiv National University, Kharkiv, Ukraine

*e-mail: gangapsh@list.ru

Abstract—We report on the study of thermal neutron flux using monitors based on mixture of Zn LiF enriched with a lithium-6 isotope at the deep underground laboratory DULB-4900 at the Ba trino Observatory. An annual modulation of thermal neutron flux in DULB-4900 is observed. Experimental evidences were obtained of correlation between the long-term thermal neutron flux variations and relative humidity of the air in laboratory. The amplitude of the modulation exceed 5% of total neutron flux.

DOI: 10.1134/S1063779616060022

Large volume detectors
(6LiF + ZnS(Ag))

Thermal flux:
 $\sim 10^{-9} - 10^{-6}$ MeV

No fully spectrometric studies yet!

